



HAL
open science

Natural gas-fueled multigeneration for reducing environmental effects of brine and increasing product diversity: Thermodynamic and economic analyses

M. Ehyaei, M. Kasaeian, Stéphane Abanades, Armin Razmjoo, Hamed Afshari, Marc Rosen, Biplab Das

► To cite this version:

M. Ehyaei, M. Kasaeian, Stéphane Abanades, Armin Razmjoo, Hamed Afshari, et al.. Natural gas-fueled multigeneration for reducing environmental effects of brine and increasing product diversity: Thermodynamic and economic analyses. *Energy Science & Engineering*, 2023, 11 (3), pp.1025-1043. 10.1002/ese3.1371 . hal-04113893

HAL Id: hal-04113893

<https://hal.science/hal-04113893>

Submitted on 1 Jun 2023

HAL is a multi-disciplinary open access archive for the deposit and dissemination of scientific research documents, whether they are published or not. The documents may come from teaching and research institutions in France or abroad, or from public or private research centers.

L'archive ouverte pluridisciplinaire **HAL**, est destinée au dépôt et à la diffusion de documents scientifiques de niveau recherche, publiés ou non, émanant des établissements d'enseignement et de recherche français ou étrangers, des laboratoires publics ou privés.

1 **Natural gas-fueled multi-generation for reducing environmental effects of brine and**
2 **increasing product diversity: Thermodynamic and economic analyses**

3
4 **M. A. Ehyaei^{1*}, M. Kasaeian², Stéphane Abanades³, Armin Razmjoo⁴, Hamed Afshari⁵**

5 **Marc A. Rosen⁶, and Bilap Das⁷**

6 ¹ Department of Mechanical Engineering, Pardis Branch, Islamic Azad University, Parids City, Iran

7 ²Department of Environmental Economics, Science and Research Branch, Islamic Azad University, Tehran, Iran

8 ³ Processes, Materials, and Solar Energy Laboratory, PROMES-CNRS, 7 Rue du Four Solaire, 66120 Font-Romeu,
9 France

10 ⁴Escola Tècnica Superior d'Enginyeria Industrial de Barcelona (ETSEIB), Universitat Politècnica de Catalunya
11 (UPC), Av. Diagonal, 647, 08028 Barcelona, Spain

12 ⁵ Food Science & Engineering Department, Faculty of Civil & Earth Resources Engineering, Islamic Azad University
13 Central Tehran Branch, Tehran, Iran

14
15 ⁶ Faculty of Engineering and Applied Science, University of Ontario Institute of Technology, 2000 Simcoe Street
16 North, Oshawa, Ontario, L1G 0C5, Canada

17 ⁷PVT Laboratory, Department of Mechanical Engineering, NIT Silchar, Assam-788010, India

18 *Corresponding author: aliehyaei@yahoo.com

19 **Abstract.** Water scarcity threatens human life and it is likely to be a main concern in the next
20 century. In this work, a novel multigeneration system (MGS) is introduced and assessed with
21 energy, exergy, and economic analyses. This multigeneration system includes a gas cycle, multi-
22 effect distillation, an absorption refrigeration cycle, a heat recovery steam generator, and
23 electro dialysis. Electro dialysis is integrated into this configuration to produce sodium hydroxide
24 and hydrogen chloride from brine to prevent its release to the environment with harmful
25 impacts. The other products are electricity, cooling, and demineralized water. For the evaluation
26 of the proposed system, one computer code is provided in engineering equation solver software.
27 For physical properties calculation, the library of this software is used. The MGS produces 614.7
28 GWh of electrical energy, 87.44 GWh of cooling, 12.47 million m³ of demineralized water, and
29 0.092 and 0.084 billion kilograms of sodium hydroxide and hydrogen chloride over a year. Energy
30 and exergy evaluations demonstrate that the MGS energy and exergy efficiencies are 31.3% and
31 18.7%, respectively. The highest and lowest value of exergy destruction rate is associated with
32 the combustion chamber and pump, respectively. The economic evaluation indicates that the net
33 present value of this proposed system is 3.8 billion US\$, while the internal rate of return and
34 payback period respectively are 0.49 and 2.1 years.

35 **Keywords:** Exergy, water shortage, Multigeneration system; Gas cycle, Economic analysis.
36
37
38

39 **Introduction**

40 Water covers 70% of the earth as lakes, rivers, seas, and oceans, but only 3% of this resource is fresh
41 water. Two-thirds of this freshwater is frozen and non-accessible for use. Thus, the fresh shortage is a
42 considerable issue for humanity [1]. According to statistical data [2], around 1.2 billion people cannot
43 access adequate water throughout the year. In addition, 2.7 billion people encounter a lack of water for
44 one month of a year and 2.4 billion people are exposed to water diseases annually, with 2 million
45 casualties each year [2].

46 According to terminology, water shortage is usually named water scarcity. Water scarcity means an
47 imbalance between the production and consumption of freshwater. It can happen throughout the year
48 or for a limited time. Water scarcity is a significant concern for humanity since freshwater is an essential
49 requirement for health and life. In addition, non-potable water is needed for agriculture, industry, and
50 energy production. This need grows as the global population increases. Other environmental and social
51 factors influence water scarcity, including climate change and living standards [3].

52 Desalination technologies have been developed for over 50 years. Early studies were conducted during
53 World War II and research has continued until now [4]. Desalination processes are classified by approach
54 [5]:

55 1) Thermal distillation

56 This method is based on evaporation and condensation to continuously purify water and separate
57 dissolved solids (DS) such as salt [5]. This method is common in the Middle East due to the cheap price of
58 oil and natural gas. This method can be divided into multi-effect distillation (MED) and multi-stage flash
59 (MSF).

60 2) Membrane separation

61 This method is based on filtration. Seawater (SW) flows through a membrane and non-dissolved solids are
62 separated from the water. This method does not require any thermal energy and only electrical energy is
63 consumed to meet the electrical energy needs of the reverse osmosis (RO) pumps. This method can be
64 divided into reverse osmosis (RO) [6] and forward osmosis (FO) [7] processes.

65 3) Other approaches

66 Several other desalination methods also exist such as humidification-dehumidification (HDH) [8],
67 membrane distillation (MD) [9], freezing, and solar stills [10].

68 When comparing thermal distillation and membrane separation, thermal separation is preferred at a large
69 scale due to lower operation and maintenance costs and the possibility to use the energy of hot exhaust
70 gas from various industries [11].

71 One of the oldest distillation methods is MED. This technology is used on a large scale and has been
72 improved in recent years. In comparison with MSF, MED is preferable due to its low-temperature
73 operation, higher capacity to produce potable water (PW), better heat transfer, and lower electrical
74 power consumption of pumps [11].

75 One of the disadvantages of the desalination process is the environmental concern of brine disposal. Brine
76 disposal methods can be classified as injection to well, surface water, and land disposal [12]. All of these
77 methods are harmful to the environment, by threatening marine life, degradation of soil and groundwater
78 quality, etc. So, the conversion of exhaust brine from the desalination plant to useful and valuable
79 materials has many economic and environmental benefits [13].

80 A gas turbine power generation system was introduced 70 years ago. Over the last 20 years, its usage has
81 increased 20-fold, especially in regions with high NG resources [14].

82 Gas turbine power generation systems have two major weaknesses [15]:

83 1) Low efficiency (~20 - 45%) due to the dissipation of exhaust hot gas to the atmosphere [16]

84 2) Significant effect of air temperature increase on gas turbine efficiency [17]

85 There are various technologies to fix these defects such as inlet air cooler systems , bottom cycles to
86 produce extra electrical power by utilizing the hot exhaust gases via a heat recovery steam generator
87 (HRSG) [18], air bottom cycles (ABCs) [19]), integration with renewable energy resources for performance
88 enhancement [20], integration with other power generation systems such as solid oxide fuel cells (SOFCs)
89 [21], multigeneration systems (MGS) for production of various products simultaneously such as hydrogen
90 [22], urea , and PW [23].

91 Thus, integration of MED with a gas cycle (GC) has benefits due to enhancing system performance. It has
92 also further benefits if the portion of the plant downstream of the MED is integrated with a system that
93 converts the brine to useful products to further increase system efficiency and reduce environmental
94 impacts.

95 Considerable research has been done on MGS, especially the integration of GCs with MED. In an early
96 work of Chacartegui et al. , a feasibility study of the integration of the GC with the MED was carried out.

97 The results showed that this integration was beneficial from energy and economic points of view.
98 Mokhtari et al. [24] performed thermoeconomic and exergy evaluations of a GC/MED/RO system. This
99 proposed system produced 79.2×10^6 kWh/year of electricity and 10.3×10^3 m³/day PW. Rensonnet et al.
100 [25] performed a thermoeconomic investigation for four different configurations including GC/RO,
101 combined cycle (CC) with RO, CC/MED, and CC/MED/RO, respectively. The configuration of CC/MED/RO
102 had the lowest unit cost at 0.15 US\$/kWh. Ahmadi et al. [26] evaluated the integration of the MED with a
103 GC (GC capacity of 48 MW). This integration produced 12294 m³/day PW with a 1.6 US\$/m³ cost. The
104 system exergy efficiency was 38.9%. In a similar study, Shakouri et al. [23] evaluated and optimized the
105 integration of GC with MED from an economic point of view. They found that the 3-effect MED is the best
106 choice with 0.51 kg/s distilled water (DW) production and 2 US\$/m³ unit product cost (UPC).

107 The integration of SOFC with GC, and MED is another interesting topic. Mohammadnia and Assadi [27]
108 evaluated a hybrid system including GC, SOFC, HRSG, and MED with a thermal vapor compressor (TVC), in
109 terms of energy, exergy, and economics. They calculated the gross output ratio (GOR), net output power,
110 distilled water production, system total product cost (TPC), and system exergy efficiency as 7.6, 3219.3
111 kW, 3.2 kg/s, 0.02 US\$/s, and 59.4%, respectively. In a similar study, Ahmadi et al. [28] performed
112 exergoeconomic optimization of a system consisting of GC, SOFC, and MED-TVC with a genetic algorithm
113 (GA). The authors determined an increase in the system exergy efficiency from 57% to 63.5% and a drop
114 in the electricity cost to 0.064 US\$/kWh.

115 Several systems were proposed as MGS for various products. Nazari and Porkhial [29] proposed an MGS
116 including GC, organic Rankine cycle (ORC), Rankine cycle (RC), and absorption refrigeration cycle (ARC).
117 This system used NG, biogas (BG), and solar energy via a parabolic trough collector (PTC), simultaneously.
118 The products of the MGS were PW, cooling, and electrical power. The system exergy efficiency and TPC
119 were 21.5%, and 77.3 US\$/h, respectively. You et al. [30] assessed an MGS including GC, MED-TVC, ORC,
120 and steam ejector refrigerator (SER) to produce PW, electricity, heating, and cooling. This MGS can
121 produce 31.2 MW of electricity, 1.1 MW of heating, 4.2 MW of cooling, and 85.9 kg/s of PW. The calculated
122 system exergy efficiency is 41.3%. In another study, Moghimi et al. [31] introduced an MGS consisting of
123 GC, HRSG, MED, and an ejector refrigerator system (ERS). This MGS produced 85.6 kg/s PW, 2 MW cooling,
124 and 30 MW electricity. The calculated system exergy efficiency is 36%.

125 Considering the previous studies, the research gap in the literature is as follows:

- 126 • Treatment of brine discharge downstream of MED to avoid environment harmfully

- 127 • Non-use of brine or converting it to useful products

128 In this article, a new MGS consisting of GC, HRSG, MED-TVC, ARC, and electro dialysis (ELECD) is proposed
129 to convert the brine to NaOH and HCl as valuable products. The system products are electricity, cooling,
130 PW, NaOH, and HCl. This MGS is powered by NG. All aspects of this new MGS are examined by energy,
131 exergy, and economic (3E) analyses. In summary, The novelties of this research are as follows:

- 132 • Presenting a new multiple production system with the aim of eliminating the environmental
133 effects of brine
- 134 • Energy, exergy , and economic analyses of the proposed system

135

136

137 **1) Modeling**

138 **2.1. System layout and description**

139 Figure 1 illustrates the layout of the proposed MGS. In the GC, NG is compressed in the booster
140 compressor (BC) (points 1&2). Then, it is reacted by pressurized air from the compressor (C) (points 3&4)
141 in the combustion chamber (CC) to produce hot gas (point 5) that rotates the gas turbine (GT) and
142 generator for electrical production (point 6). Then, it flows through the HRSG to produce superheated
143 steam (point 7). After, it flows through the ARC to supply the electricity required by the generator of the
144 ARC and produce cooling (point 8). In the steam cycle (SC), the pressurized water (point 11) exchanges
145 the heat with exhaust GT hot gas to produce the superheated steam (point 9). The superheated steam is
146 injected into the MED/TVC for DW production from the seawater (point 9). After, it goes to pump 1 (P1)
147 (point 10).

148 Figure 2 depicts the layout of the MED. The MED converts the SW (point 12) to DW (point 13) and
149 dissipated brine (point 14). This system operates based on successive evaporation and condensation and
150 has several stages named effects and one condenser. In the MED, TVC works by the superheated steam
151 (point 19: motive steam) and it pressurizes the part of water vapor generated in the last effect (entrained
152 steam). Produced steam supplies the energy needed by MED.

153 In the first effect of the MED, the exit steam of the TVC goes in the tubes to evaporate the SW sprayed on
154 them in the first effect. The steam in the tubes is condensed. The evaporated SW in the first effect is
155 collected with evaporated brine in the flash boxes and goes into the tubes of the second effect. In flash

156 boxes, a small pressure drop causes a small portion of brine to evaporate. This process continues until the
157 last effect. It is important to mention that number of effects is clarified based on the requested capacity
158 of DW. To improve the performance of the MED, the SW is preheated in the preheater with distillate vapor
159 (DV) in each effect

160 Part of the dissipated brine is injected into the ELECD and it is converted to NaOH and HCl by electrolyzing
161 the SW using electricity. This MGS has several subsystems: GC, SC, MED, ARC, and ELECD. The products
162 are electricity, cooling, DW, NaOH, and HCl (points 15 and 16). The connections between the subsystems
163 are depicted in Figure 3.

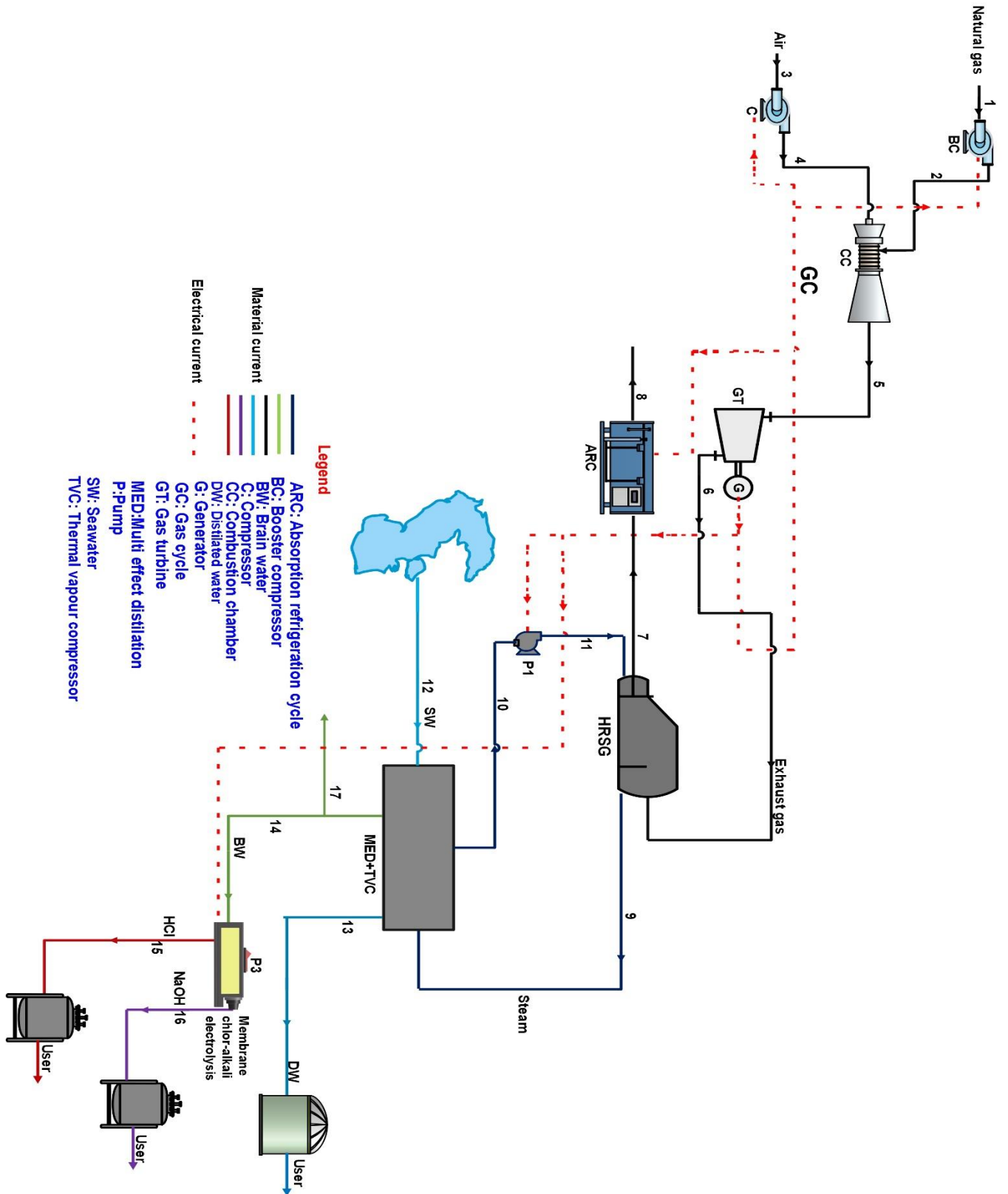
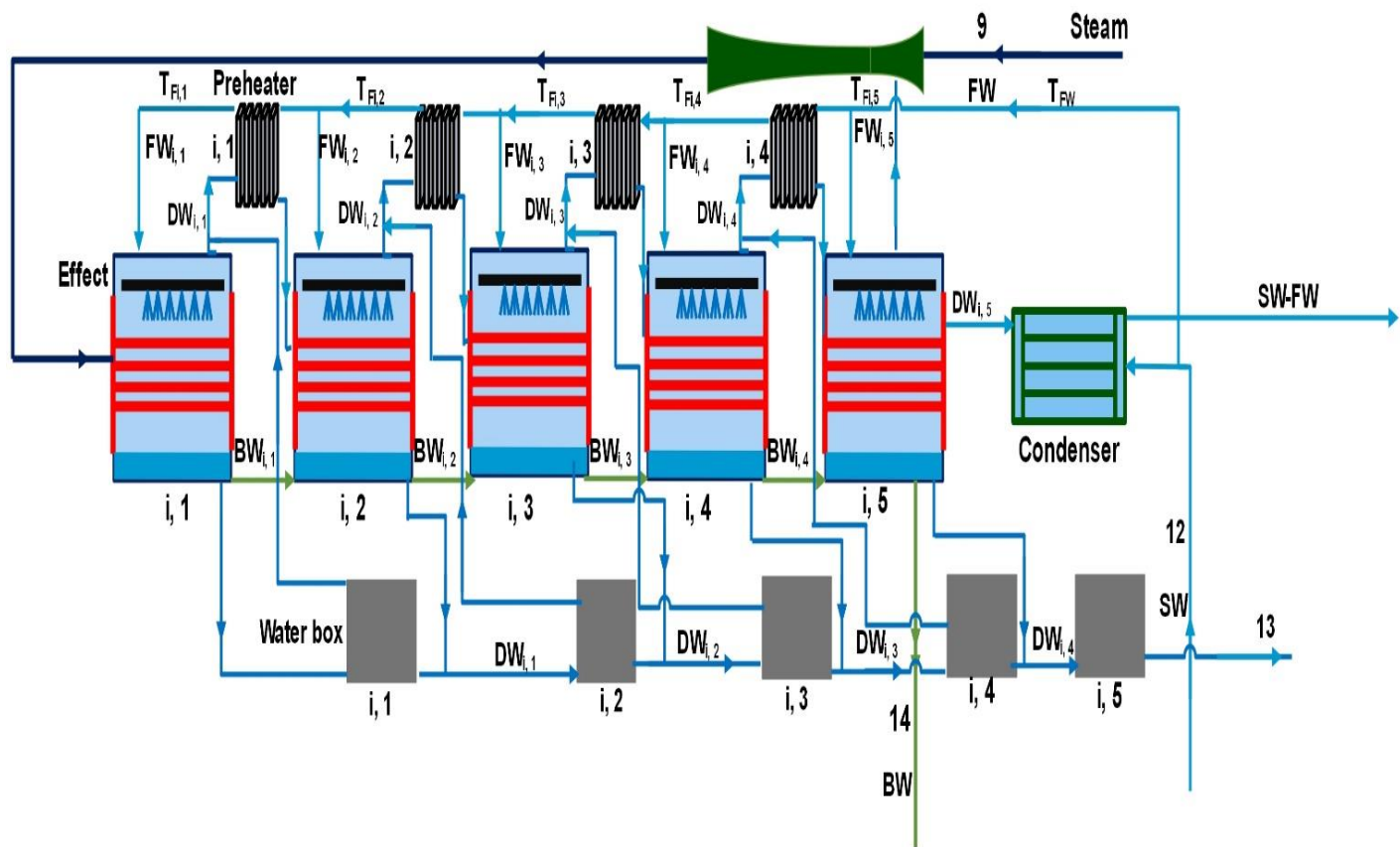


Figure 1. The layout of the proposed MGS (stream numbers are identified in the text)

164

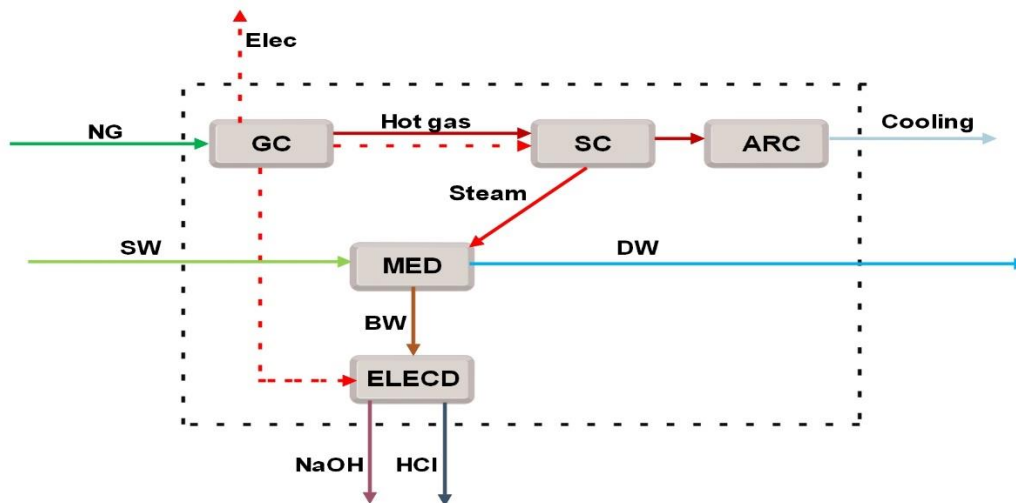
165



166

167

Figure 2. Configuration of the MED



168

169

170

Figure 3. General schematic of the studied system

171 For the modeling, the following assumptions are considered [32]:

- 172 1. The reference environment temperature and pressure are 15 °C and 101.3 kPa, respectively.
 173 2. Heat loss is ignored.
 174 3. The thermodynamic processes in the C and GT are polytropic.
 175 4. Kinetic and potential energies are ignored.
 176 5. The efficiency of the CC is 98%.
 177 6. For the BC, C, and GT, the polytropic efficiencies are respectively 85%, 85%, 78%.
 178 7. DV and brine have an effective temperature at the exit.
 179 8. The DV is slightly superheated and completely pure.
 180 9. The overall heat transfer coefficients in the MED are a function of temperature.
 181 10. The temperature difference in each effect is assumed equal.
 182 11. The feed water in the MED is distributed equally.

183 **2.2. Energy and Mass balance**

184 **2.2.1. Gas cycle, Steam cycle, and Absorption refrigeration cycle**

185 Mass and energy balance equations are written as follows [33]:

186

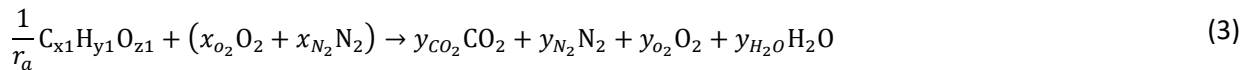
$$\sum_{in} \dot{m} = \sum_{out} \dot{m} \quad (1)$$

187

$$\dot{Q} - \dot{W} + \sum_{in} \dot{m} \left(h + \frac{V^2}{2} + gZ \right) = \sum_{out} \dot{m} \left(h + \frac{V^2}{2} + gZ \right) \quad (2)$$

188

189 The combustion reaction in the CC can be written as follows:



$$y_{CO2} = \frac{x_1}{r_a} \quad (4)$$

$$y_{N2} = x_{N2} \quad (5)$$

$$y_{H2O} = x_{H2O} + \frac{y_1}{2r_a} \quad (6)$$

$$y_{O2} = z_1 + x_{O2} - \frac{x_1}{r_a} - \frac{y_1}{4r_a} \quad (7)$$

$$r_a = \frac{n_{Air}}{n_{Fuel}} \quad (8)$$

190

191 where x_i and y_i specify the mass and mole fractions of i and r_a depicts the air/fuel ratio. The NG molar
 192 composition used in the GC is presented in Table 1 [34].

193 Table 1. Molar composition of NG

Component	Mixture (%molar)
CH ₄	80.4
C ₂ H ₆	8.5
C ₃ H ₈	4.1
C ₄ H ₁₀	4.8
CO ₂	1.1
N ₂	1.1

194

195 The mass and energy balance equations for each component of the GC and SC are presented in Table 2.

196 Table 2. Mass and energy rate balance equations for the component of the GC and SC

No.	Component	Mass balance	Energy balance
GC			
1	Compressor	$\dot{m}_3 = \dot{m}_4$	$\dot{W}_C = \frac{\dot{m}_3(h_4 - h_3)}{\eta_C}$
2	Booster compressor	$\dot{m}_1 = \dot{m}_2$	$\dot{W}_{BC} = \frac{\dot{m}_1(h_2 - h_1)}{\eta_{BC}}$
3	Combustion chamber	$\dot{m}_2 + \dot{m}_4 = \dot{m}_5$	$\eta_{CC}(\dot{m}_4 h_4 + \dot{m}_2 h_2 + \dot{m}_2 LHV) = \dot{m}_5 h_5$
4	Gas turbine	$\dot{m}_5 = \dot{m}_6$	$\dot{W}_{GT} = \dot{m}_5(h_5 - h_6)\eta_{GT}$
SC			
5	Pump	$\dot{m}_{10} = \dot{m}_{11}$	$\dot{W}_P = \frac{\dot{m}_{10}(h_{11s} - h_{10})}{\eta_P}$
6	HRS	$\dot{m}_6 = \dot{m}_7$ $\dot{m}_9 = \dot{m}_{11}$	$\dot{m}_6(h_6 - h_7)\eta_{HX} = \dot{m}_9(h_9 - h_{11})$
ARC			
7	ARC	$\dot{m}_7 = \dot{m}_8$	$\dot{m}_7(h_7 - h_8)COP = \dot{Q}_{Cooling}$

197

198 The COP and η mean the coefficient of performance (ARC) and efficiency. Subscript HX means heat
 199 exchanger.

200 **2.2.2. Multi-effect distillation**

201 The effect of temperature difference is considered as follows [35]:

$$T_i - T_{i-1} = \Delta T \quad (i = 2, \dots, N) \quad \text{in } \Delta T = \frac{T_1 - T_N}{N - 1} \quad (9)$$

202

203 Here, T and N denote temperature and effects number. The subscript i specifies the number of effects.

204 The temperature of the vapor inside the effects should be considered as follows [36]:

205

$$T_{vi} = T_i - BPE \quad (10)$$

206 Here, subscript v shows vapor. Boiling point elevation (BPE) is a factor that determines the salt effect on
 207 evaporation [36].

208 The temperature in the flash boxes can be determined as follows due to non-equilibrium allowance
 209 (NEA)[37]:

$$T_{i'} = T_{vi} + NEA \quad (11)$$

210 where NEA is determined by [37]:

$$NEA = \frac{0.33(T_{vi-1} - T_{vi})}{T_{vi}} \quad (12)$$

211 The SW mass flow rate in each effect is calculated as follows [35]:

$$\dot{m}_{SW,i} = \frac{\dot{m}_{SW}}{N} \quad (13)$$

212 Mass and concentration balance relations are as follows [38, 39]:

$$\dot{m}_{DW,i} = \dot{m}_{BW,i-1} + \dot{m}_{SW,i} - \dot{m}_{BW,i} \quad (14)$$

$$\dot{m}_{SW,i}x_{SW,i} + \dot{m}_{BW,i-1}x_{BW,i-1} = \dot{m}_{BW,i}x_{BW,i} \quad (15)$$

213 where x denotes salt concentration.

214 The energy balance equation for each effect can be calculated as follows [38, 39]:

$$\dot{m}_{DW,i}L_N = \left[\dot{m}_{DW,N-1} + \sum_{l=1}^{N-2} (\dot{m}_{DW,r} + \dot{m}_{DW,i})ff - (N-1)\dot{m}_{SW,N} \right] L_{N-1} - \dot{m}_{SW}C_p(T_N - T_{SW,i}) + \dot{m}_{BW,N-1}C_p\Delta T \quad (16)$$

215

216 Here, ff and L denote flashing fraction and latent heat, while subscript r means entrained steam.

217 The overall surface area of each effect, condenser, and preheater is calculated with the following relations

218 [39, 40]:

$$A_{effects} = \frac{[(\dot{m}_{DW,N-1} + \dots + \dot{m}_{DW,N-2} + \dot{m}_{DW,r})ff - (N-1)ff\dot{m}_{SW,N}]L_{N-1}}{U_{effects}(T_{v,N-1} - T_N)} \quad (17)$$

$$A_{cond} = \frac{[(\dot{m}_{SW} + (\dot{m}_{DW,r}\dot{m}_{DW,1} + \dots + \dot{m}_{DW,N-1}))ff]L_N}{U_{cond}LMTD_{cond}} \quad (18)$$

$$A_{ph} = \frac{N\dot{m}_{SW,N}[T_{SW,N} - T_{SW,N+1}]}{U_{ph}LMTD_{ph}} \quad (19)$$

219

220 Subscripts $cond$ and ph represent respectively condenser and preheater of the MED.

221 The coefficient U for the effects, $cond$, and ph of the MED can be expressed respectively as follows [39,

222 40]:

$$U_{effects} = 1939.4 + 1.40562T_{effect} - 2.07525 \times 10^{-2}T_{effect}^2 + 2.3186 \times 10^{-3}T_{effect}^3 \quad (20)$$

$$U_{cond} = 1617.5 + 0.1537T_{cond} - 0.1825T_{cond}^2 + 8.026 \times 10^{-5}T_{cond}^3 \quad (21)$$

$$U_{ph} = 14182.51642 + 11.383865T_{v,N} + 13.381501T_{SW,N+1} \quad (22)$$

223

224 The ratio of entrained steam ($\dot{m}_{dv,N}$) to motive steam (\dot{m}_m or \dot{m}_9) can be expressed as follows [41]:

$$Ra = \frac{\dot{m}_m}{\dot{m}_{DV,N}} \quad (23)$$

225 Ra is calculated by [38]:

$$Ra = 0.235 \frac{P_S^{1.19}}{P_{DV,N}^{1.04}} \left(\frac{P_m}{P_{DV,N}} \right)^{0.015} \quad (24)$$

226 Here, P denotes pressure.

227 The TVC outlet stream is described as follows [38]:

$$\dot{m}_s = \dot{m}_{DV,N} + \dot{m}_m \quad (25)$$

228 where subscript s represents the outlet steam of the TVC.

229 For evaluation of the MED, two factors should be calculated named recovery gained output ratio (*GOR*)
 230 and ratio (*RR*):

$$GOR = \frac{\dot{m}_{DW}}{\dot{m}_m} \quad (26)$$

$$RR = \frac{\dot{m}_{DW}}{\dot{m}_{SW}} \quad (27)$$

231

232 2.2.3. Electrodialysis

233 In the ELECD, the following reaction takes place driven by electricity [42]:



234 The precondition of this reaction in ELECD is that the salt concentration should exceed 26%. This sub-
 235 system requires 0.73 kWh of electrical energy per kilogram of NaOH.

236 2.2.4. Energy efficiency evaluation

237 The energy efficiency of the GC, GC/SC/MED/ARC, and system are considered by the following relations:

$$\eta_{GC} = \frac{\dot{W}_{GT} - \dot{W}_C - \dot{W}_{BC}}{\dot{m}_1 LHV} \quad (29)$$

$$\eta_{GC/SC/MED/ARC} = \frac{\dot{W}_{GT} - \dot{W}_C - \dot{W}_{BC} - \dot{W}_{P1} + \dot{m}_7(h_7 - h_8)COP + \dot{m}_{13}h_{13}}{\dot{m}_1 LHV} \quad (30)$$

$$\eta_{sys} = \frac{\dot{W}_{GT} - \dot{W}_C - \dot{W}_{BC} - \dot{W}_{P1} - \dot{W}_{ELECD} + \dot{m}_7(h_7 - h_8)COP + \dot{m}_{13}h_{13} + \dot{m}_{15}h_{15} + \dot{m}_{16}h_{16}}{\dot{m}_1 LHV} \quad (31)$$

238

239 2.3. Exergy analysis

240 Specific exergy is divided into four kinds (chemical, kinetic, physical, and potential) as considered below
 241 [43, 44]:

$$\Psi = \sum x_i \Psi_{chi} + \frac{V^2}{2} + gz + (h - h_0) - T_0(s - s_0) + T_0 \sum x_i R_i \ln y_i \quad (32)$$

242

243 Here, x and Ψ denote mass fraction and specific exergy respectively. Also, g is the gravitational
 244 acceleration, V and z are velocity and height, y and s denote mole fraction and specific entropy, and
 245 subscripts 0, i , and ch denote dead state, species, and chemical. Table 3 shows the EDR for each
 246 component of the MGS.

247 Table 3. EDR equations for different components

No.	Component	EDR
1	Compressor	$\dot{m}_3\Psi_3 + \dot{W}_C - \dot{m}_4\Psi_4$
2	Booster compressor	$\dot{m}_1\Psi_1 + \dot{W}_{BC} - \dot{m}_2\Psi_2$
3	Combustion chamber	$\dot{m}_2\Psi_2 + \dot{m}_4\Psi_4 - \dot{m}_5\Psi_5$
4	Gas turbine	$\dot{m}_5\Psi_5 - \dot{m}_6\Psi_6 - \dot{W}_{GT}$
5	Pump 1	$\dot{m}_{10}\Psi_{10} + \dot{W}_P - \dot{m}_{11}\Psi_{11}$
6	HRSG	$\dot{m}_6(\Psi_6 - \Psi_7) + \dot{m}_{11}(\Psi_{11} - \Psi_9)$
7	ARC	$\dot{m}_7(\Psi_7 - \Psi_8) - \dot{Q}_{ARC}(1 - \frac{T_0}{T_{ARC}})$
8	MED/TVC	$\dot{m}_9\Psi_9 + \dot{m}_{12}\Psi_{12} - \dot{m}_{10}\Psi_{10} - \dot{m}_{13}\Psi_{13} - \dot{m}_{14}\Psi_{14}$
9	ELECD	$\dot{m}_{14}\Psi_{14} + \dot{W}_{ELECD} - \dot{m}_{15}\Psi_{15} - \dot{m}_{16}\Psi_{16}$

248

249 2.3.1. Exergy efficiency evaluation

250 The exergy efficiency of the GC, GC/SC/MED/ARC, and the system can be written as follows:

$$\varepsilon_{GC} = \frac{\dot{W}_{GT} - \dot{W}_C - \dot{W}_{BC}}{\dot{m}_1\Psi_1} \quad (33)$$

$$\varepsilon_{GC/SC/MED/ARC} = \frac{\dot{W}_{GT} - \dot{W}_C - \dot{W}_{BC} - \dot{W}_{P1} + \dot{Q}_{ARC}(1 - \frac{T_0}{T_{ARC}}) + \dot{m}_{13}\Psi_{13}}{\dot{m}_1\Psi_1} \quad (34)$$

$$\varepsilon_{Sys} = \frac{\dot{W}_{GT} - \dot{W}_C - \dot{W}_{BC} - \dot{W}_{P1} - \dot{W}_{ELECD} + \dot{Q}_{ARC}(1 - \frac{T_0}{T_{ARC}}) + \dot{m}_{13}\Psi_{13} + \dot{m}_{15}\Psi_{15} + \dot{m}_{16}\Psi_{16}}{\dot{m}_1\Psi_1} \quad (35)$$

251

252 2.4. Economic Investigation

253 The annual income (AI) of this proposed system is calculated based on product sales over a year minus
 254 the cost of the NG consumed in the MGS and is calculated as follows [45, 46]:

$$AI = Y_{elec}c_{elec} + Y_{cooling}c_{cooling} + Y_{DW}c_{DW} + Y_{NaOH}c_{NaOH} + Y_{HCl}c_{HCl} - Y_{NG}c_{NG} \quad (36)$$

255 Here, c represents products specific costs which can be found in Table 4, and Y denotes the annual
 256 products of the MGS [46-48]. Subscript elec denotes electricity. Note that the monetary values used in
 257 this article are 2021 US dollars.

258 Table 4. Specific costs of products and fuel

Quantity	Unit	Specific cost value	Ref.
Products			
Electricity	US\$/kWh	0.13	[49]
Cooling	US\$/kWh	0.056	[50]
Demineralized water	US\$/m ³	5.71	[51]
NaOH	US\$/kg	0.73	[52]
HCl	US\$/kg	0.336	[53]
Fuel			
Natural gas	US\$/kWh	0.064	[50]

259

260 The purchased equipment cost (PEC) of each component is presented in Table 5.

261 Table 5. Investment and installation costs of components

Component	PEC (US\$)	Ref	
Compressor	$\frac{44.71\dot{m}_3}{0.95 - \eta_C} \left(\frac{P_4}{P_3}\right) \ln\left(\frac{P_4}{P_3}\right)$	[54]	
Booster compressor	$\frac{44.71\dot{m}_1}{0.95 - \eta_{BC}} \left(\frac{P_2}{P_1}\right) \ln\left(\frac{P_2}{P_1}\right)$	[54]	
Combustion chamber	$\frac{28.98\dot{m}_4}{0.995 - \frac{P_5}{P_4}} (1 + \exp(0.015(T_5 - 1540)))$	[54]	
Gas turbine	$\left(\frac{301.45\dot{m}_5}{0.94 - \eta_{GT}}\right) \ln\left(\frac{P_5}{P_6}\right) (1 + 0.025(T_5 - 1570))$	[54]	
ARC	$1.14(14740.2095(\dot{Q}_{ARC})^{-0.6849} + 3.29)$	[55, 56]	
HRSG	$4745\left(\frac{\dot{m}_{11}(h_9)}{\log(T_6 - T_7)}\right)^{0.8} + 11820\dot{m}_{11} + 685\dot{m}_1$	[57]	
Pump	$3540(\dot{W}_P)^{0.71}$	[57]	
MED	TVC	$16.14 \times 989 \times \dot{m}_9 \times \left(\frac{T_m}{P_m}\right)^{0.05} P_e^{-0.75}$	[58]

	Effects	$201.67\dot{Q} \times LMTD^{-1} dp_{sw}^{0.15} dp_s^{-0.15}$	[58]
	Condenser	$430 \times 0.582 \times \dot{Q} LMTD^{-1} dp_{sw}^{0.01} dp_s^{-0.1}$	[58]
ELECD		$1000 \dot{W}$	[42]

262

263 According to the method explained in ref [59], the total capital investment (TCI) is divided into three
 264 categories: direct cost (DC), indirect cost (IC), and other costs (OC).

265 The effect of the inflation rate on the TCI is shown below [60]:

$$TCI_n = TCI_0(1 + i)^n \quad (37)$$

266

267 Here, n and i respectively are the number of years and the inflation rate (3.1%) [61]. The operation and
 268 maintenance cost (OMC) is calculated based on 3% of the TCI [45, 46].

269 So, the total cost (TC) can be written as follows [59]:

$$TC = TCI_n + OMC \quad (38)$$

270

271 The simple payback period (SPP) can be calculated by [45, 46]:

$$SPP = \frac{TC}{AI} \quad (39)$$

272 and the payback period (PP) as [45, 46]:

$$PP = \frac{\ln\left(\frac{AI}{AI - r \cdot TC}\right)}{\ln(1 + r)} \quad (40)$$

273

274 where r denotes the discount factor (3%) [45, 46].

275 NPV can be expressed as follows [45, 46]:

$$NPV = AI \frac{(1 + r)^N - 1}{r(1 + r)^N} - TC \quad (41)$$

276 where N presents the project lifetime (25 years) [59].

277 The Internal rate of return (IRR) can be calculated by [46, 62]:

$$IRR = \frac{AI}{TC} \left[1 - \frac{1}{(1 + IRR)^N} \right] \quad (42)$$

278

279 **2) Results and discussion**

280 For the MGS a computer code was written in the Engineering Equation Solver (EES). For the physical and
 281 thermodynamic properties of different flows (air, hydrogen, steam, SW, brine, DW, NaOH, HCl, NG, and
 282 hot exhaust gas), the existing library in EES was used. Table 6 shows the input data for the computer code.

283 Figure 4 shows a flowchart of the procedure followed by the developed code.

284

Table 6. Input data for the computer code

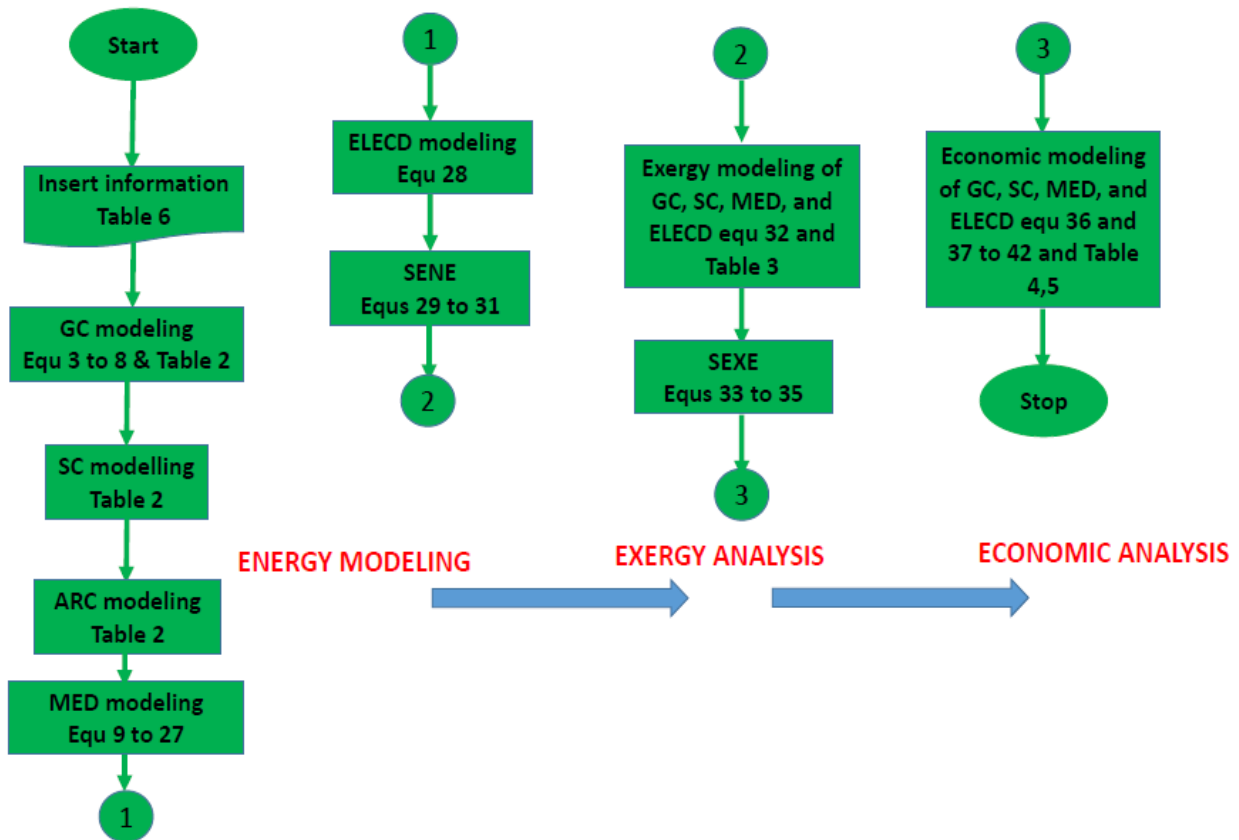
Parameter	Definition	Unit	Values
$\frac{P_4}{P_3}$	Compressor pressure ratio	-	11.1
r_a	Air/fuel ratio	-	3.1
\dot{m}_1	Fuel mass flow rate in BC	kg/s	9.316
COP	ARC coefficient of performance	-	0.8
TBT	Top brine temperature	°C	63.6
BBT	Bottom brine temperature	°C	48.6
x_{12}	Seawater salt concentration	-	40.84
x_{14}	Brine salt concentration	-	70
T_{12}	Seawater temperature	°C	30
N	Number of effects	-	5
T_1	Inlet fuel temperature of booster compressor	°C	10
T_3	Inlet air temperature of the compressor	°C	15
P_{10}	Inlet pump pressure in SC	kPa	101.3
P_{11}	Outlet pump pressure in SC	kPa	1600
Sources: [23, 63-65].			

285

286

287

288



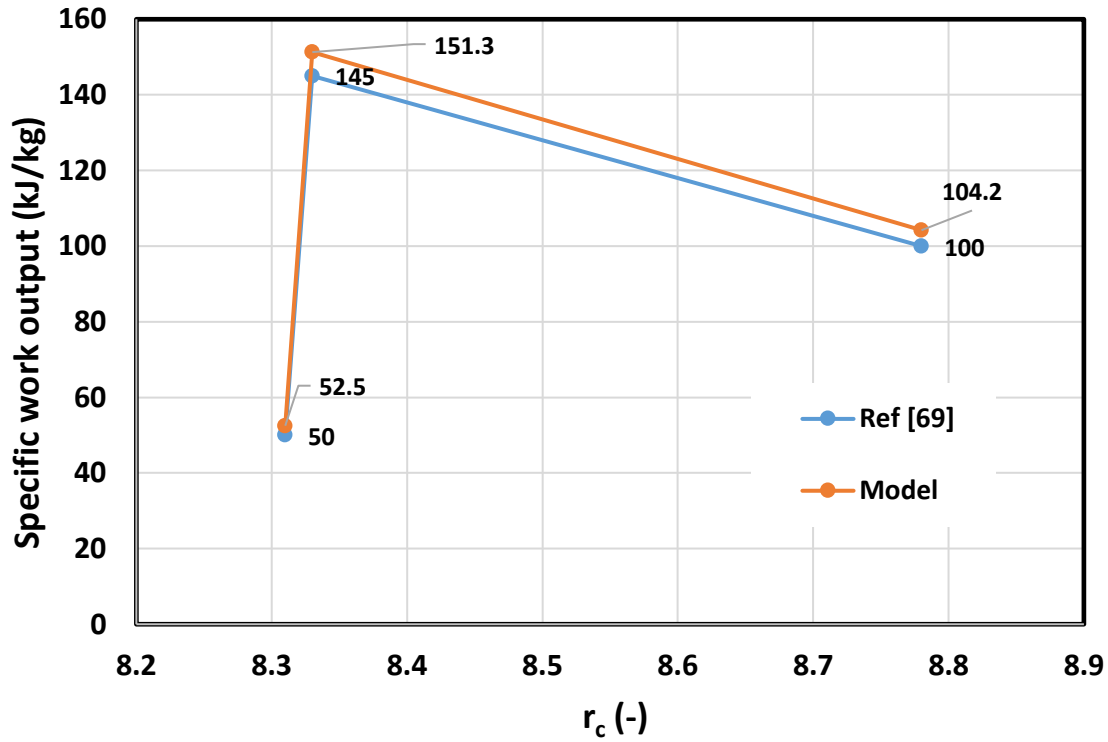
290

291

Figure 4. Flowchart of the developed code

292 **3.1. Model validation**

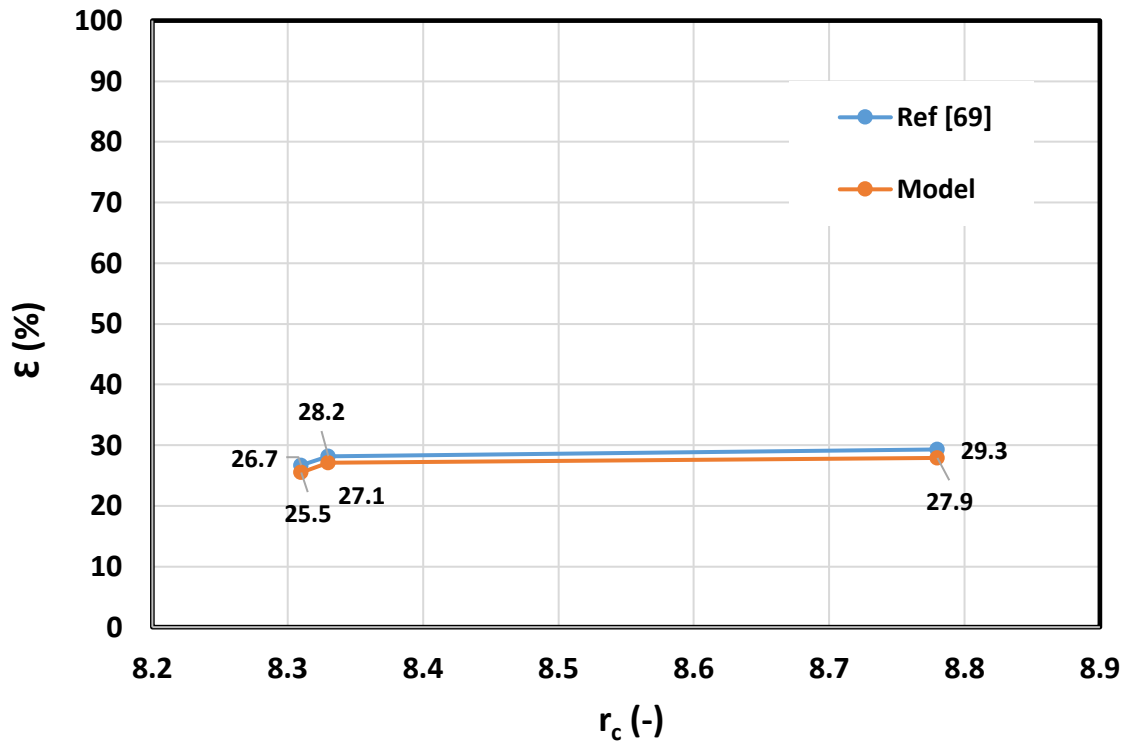
293 It is important to validate the results of energy analysis both theoretically and experimentally. For
 294 validation of the GC, Ref [66] is used, in which the GE-F5 gas cycle is considered. Figure 5 shows the
 295 comparison of the model results and the results from Ref [66]. In Figure 5, the specific work output of the
 296 GC model is compared with the results of Ref [66] for three compression ratios of the compressor. The
 297 difference is around 4%. The comparison between the GC exergy efficiency of the model and the results
 298 from Ref [66] is depicted in Figure 6 for three compression ratios of the compressor. Similar to Figure 6,
 299 the difference is around 4%.



300

301

Figure 5. Comparison of specific work output between the model and Ref [66] for the GC



302

303

Figure 6. Comparison of exergy efficiency between the model and Ref [66] for the GC

304 For the HRSG validation, Ref [67] is used, in which the pinch temperature, condenser, and boiler
305 pressures are 30 K, 0.03, and 16 bar, respectively. The validation of the model confirms that the energy
306 efficiency is 25% with a combustion chamber (CC) temperature of 1375 K. The obtained value by the
307 model is 24.1%. The calculated difference is 3.6%.

308 For validation of the MED, the cycle presented in Ref [23] is considered, as it is similar to the MGS
309 proposed in this article. Table 7 shows the results of a comparison between the MED of Ref [23] and the
310 proposed model. The difference is less than 4.3% for all comparisons.

311 Table 7. Results of comparison between the MED of Ref [23] and the model proposed in this work

Parameters	Model	Ref [23]	Error (%)
\dot{m}_9	0.109	0.114	4.3
\dot{m}_{13}	1.049	1.078	2.6
\dot{m}_{12}	5.36	5.51	2.7
\dot{m}_{14}	1.21	1.18	2.5

312

313 Since the ELECD power consumption is calculated based on real conditions, a validation of this subsystem
314 is not needed.

315 3.2. Results of energy and exergy analyses

316 The thermodynamic properties in each stream of the proposed MGS are shown in Table 8. The
317 specification of the MED is presented in Table 9. Table 10 shows the electricity produced and consumed
318 by various components and net electrical power produced by the MGS, as well as cooling production by
319 the ARC. The annual products of the MGS are presented in Table 11. The MGS produces 614.7 GWh of
320 electrical energy, 97.44 GWh of cooling, 0.092 million tonnes of NaOH, 0.084 million tonnes of HCl, and
321 12.48 million m³ of DW throughout the year. The ratio of cooling to electrical energy is equal to 15.8%.
322 The ratio of cooling to electrical power is 15.8%.

323

324

325

326

327

Table 8. Thermodynamic properties for each flow

Stream no.	\dot{m} (kg/s)	T (K)	P (kPa)	h (kJ/kg)	Ψ (kJ/kg)
1	9.316	283.2	101.3	554.9	47720.9
2	9.316	544.7	1124	1574.0	48209.6
3	610.6	288.2	101.3	288.5	6.0
4	610.6	665.2	1124	676.3	350.0
5	619.9	1138	1102	1396.0	776.2
6	619.9	759	106	867.5	241.6
7	619.9	358.1	103.8	375.5	29.1
8	619.9	338.2	101.3	353.5	23.1
9	87.7	739	1600	3397.0	1255.1
10	87.7	373.1	101.3	419.0	44.1
11	87.7	378.1	1600	441.3	50.4
12	1923	303.2	101.3	118.7	1.9
13	433.6	321.1	101.3	200.5	7.3
14	66.83	321.8	101.3	185.2	10.5
15	2.918	321.8	101.3	705.2	208.4
16	3.202	321.8	101.3	705.2	571.6
17	601.4	321.8	101.3	185.2	10.5

328

329

Table 9. Specifications of the MED

Parameter	Unit	1	2	3	4	5
A_{ph}	m^2	25012	25655	26989	28346	29782
$A_{effects}$	m^2	367.9	370.2	372.8	375.6	
BPE	$^{\circ}C$	0.49	0.53	0.57	0.63	0.7
T_b	$^{\circ}C$	63.6	59.8	56.1	52.3	48.6
T_{dv}	$^{\circ}C$	63.1	59.3	55.5	51.7	47.9
T_f	$^{\circ}C$	61.6	57.8	54	50.2	46.4
U_{effect}	W/m^2K	2644	2528	2434	2350	2277
U_{ph}	W/m^2K	15675	15581	15487	15392	
P	kPa	23	19.3	16.2	13.4	11.1

330

331

332

333

334 Table 10. The electrical power produced and consumed by components and net electrical power
 335 productions of the MGS, as well as, cooling production by ARC

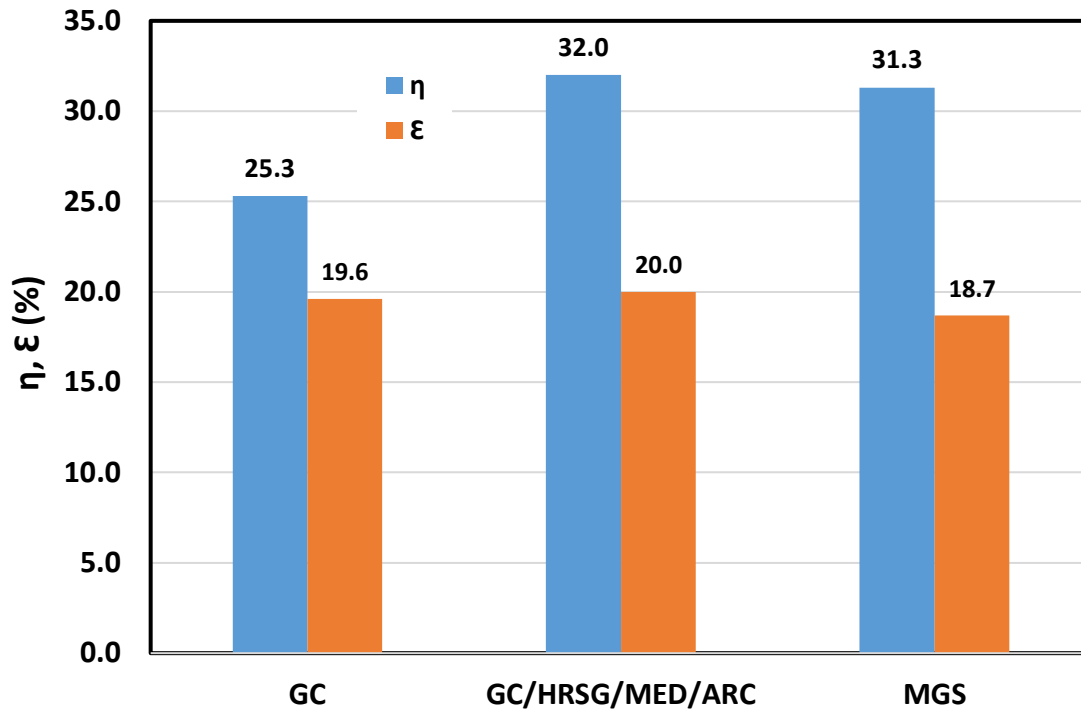
Parameter	Unit	Value
\dot{W}_C	MW	231.20
\dot{W}_{BC}	MW	9.49
\dot{W}_{GT}	MW	327.9
\dot{W}_{P1}	MW	1.95
\dot{W}_{ELECTD}	MW	8.41
\dot{W}_{net}	MW	76.83
\dot{Q}_{ARC}	MW	10.93
<i>GOR</i>	-	9.8
<i>RR</i>	-	0.23
$A_{effects,tot}$	m ²	135783
$A_{effects,ave}$	m ²	27157
$A_{condenser}$	m ²	9316
$A_{ph,tot}$	m ²	1486
$A_{MED,tot}$	m ²	146585

336 Table 11. Annual products of the MGS

Parameter	Unit	Value
Elec energy	GWh	614.70
Cooling	GWh	87.44
NaOH	million tonne	0.092
HCl	million tonne	0.084
DW	million m ³	12.48

337

338 Figure 7 shows the GC, GC/HRS/G/MED/ARC, and system energy and exergy efficiencies. By adding the
 339 MED and ARC to GC, the system energy efficiency (ENE) is increased from 25.3% to 32%, while adding the
 340 ELECD slightly decreased the system ENE from 32% to 31.3%. The reason for this increase is that the ELECD
 341 consumes a high amount of electrical energy and products of this subsystem (in the form of enthalpy of
 342 products) cannot supply its electrical power consumption. The exergy efficiency of the GC increases by
 343 adding MED/ARC from 19.6% to 20%. This increase is not considerable. Similar to system ENE, adding the
 344 ELECD decreases the exergy efficiency from 20% to 18.7% for the same reason explained previously.



345

346

Figure 7. GC, GC/MED/ARC, and system energy and exergy efficiencies

347

348

349

350

351

352

353

The EDR percentage for each component of the MGS is presented in Figure 8. The highest percentage of EDR is related to CC and MED due to combustion reaction taking place in the CC and phase change (water to vapor and vice versa) taking place in the MED. After these two components, C features the highest EDR due to the electrical power consumption of C which is summed with the EDR (row 1 of Table 3). P1 features the lowest percentage of the EDR due to the low mass flow rate of water through it and a minor difference between inlet- and outlet-specific exergies of P1. Another low percentage of EDR is related to GT since this component produces electrical power which is subtracted from the EDR.

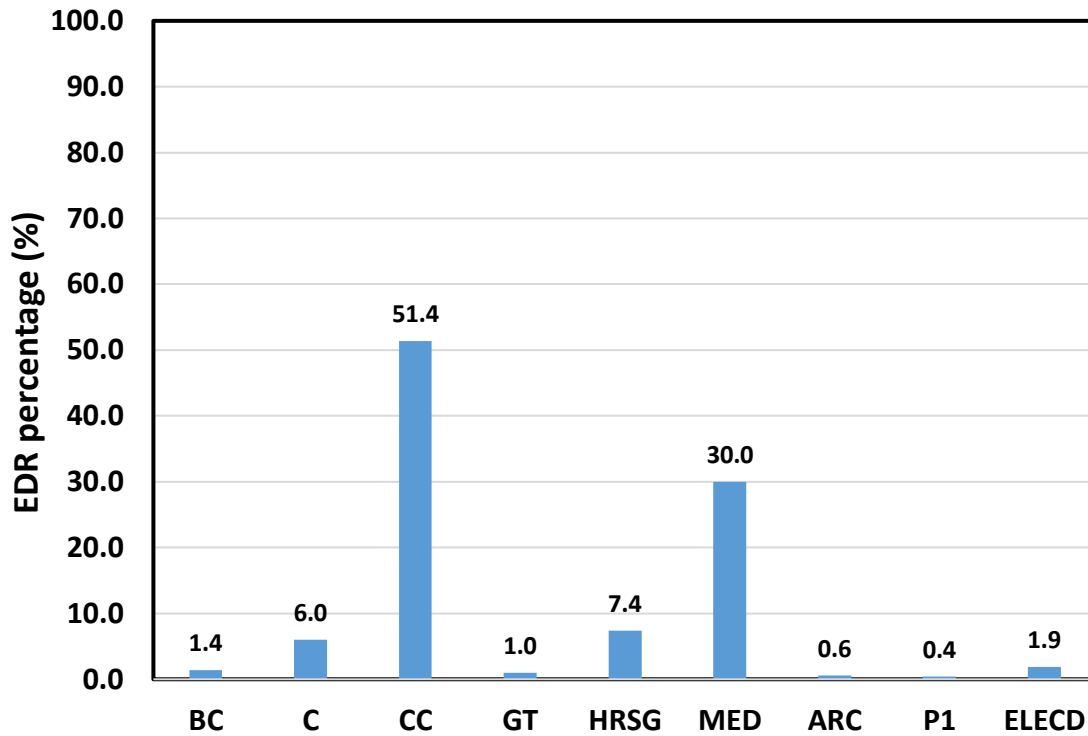


Figure 8. EDR percentage for each component of the MGS

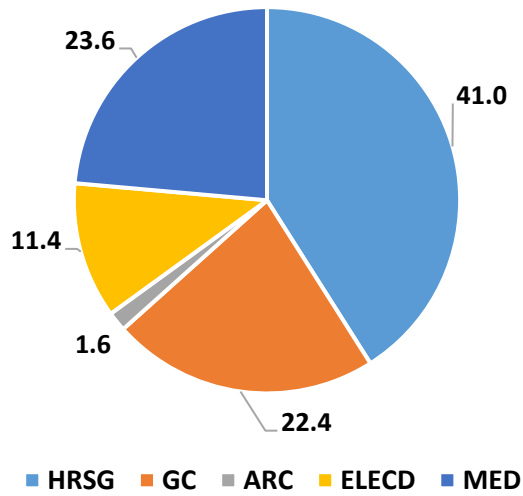
354

355

356 **3.3. Economic survey results**

357 Figure 9 shows the percentage of TC for each subsystem. The highest and lowest percentages of TC are
 358 related to HRS and ARC, respectively. The MED and GC represent 23.6% and 22.4% of TC, respectively.

359



360

361

Figure 9. Percentage of the TC for each subsystem

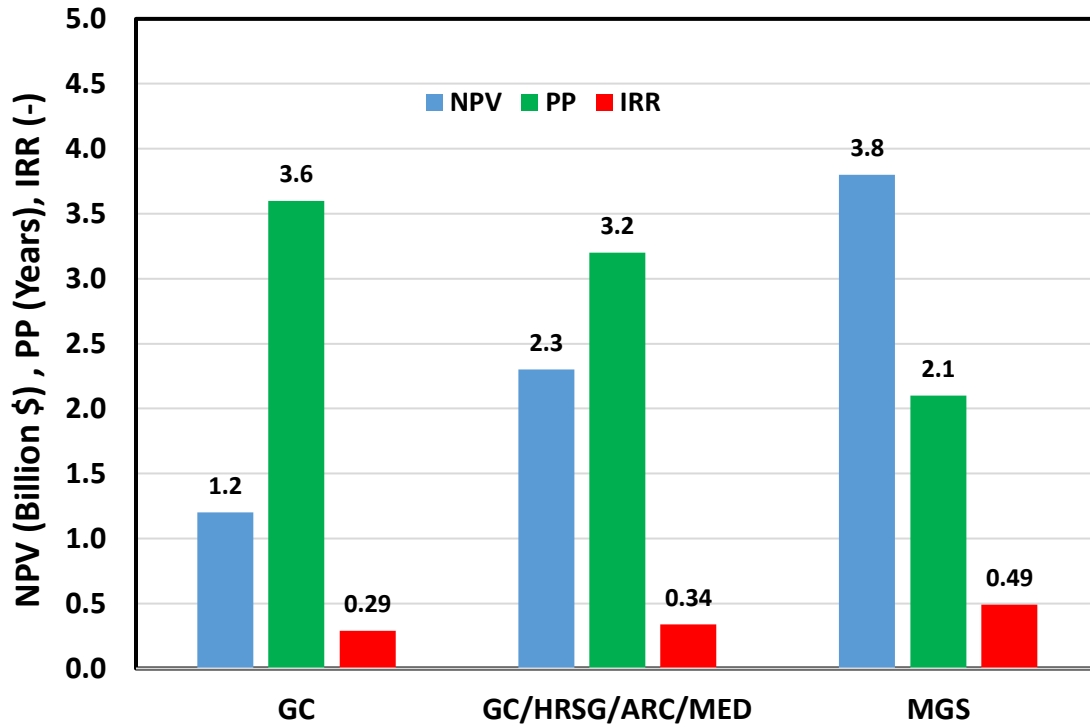
362

Figure 11 shows the NPV, PP, and IRR for three cases, including GC, GC/HRSR/ARC/MED, and the total system. Adding HRSR, ARC, and MED to GC increases the NPV from 1.2 to 2.3 billion US\$. IRR also increased from 0.29 to 0.34. PP decreased from 3.6 to 3.2 years. This can be justified because the economic values of extra products (cooling, DW) overcome the extra cost due to the addition of MED, HRSR, and ARC.

367

By adding the ELECD to the previous case, the MGS becomes more economically viable. The NPV and IRR increased by around 65% and 44%, respectively, and PP decreased from 3.2 to 2.1 years. The previous justification for this result also applies in this case.

370



371

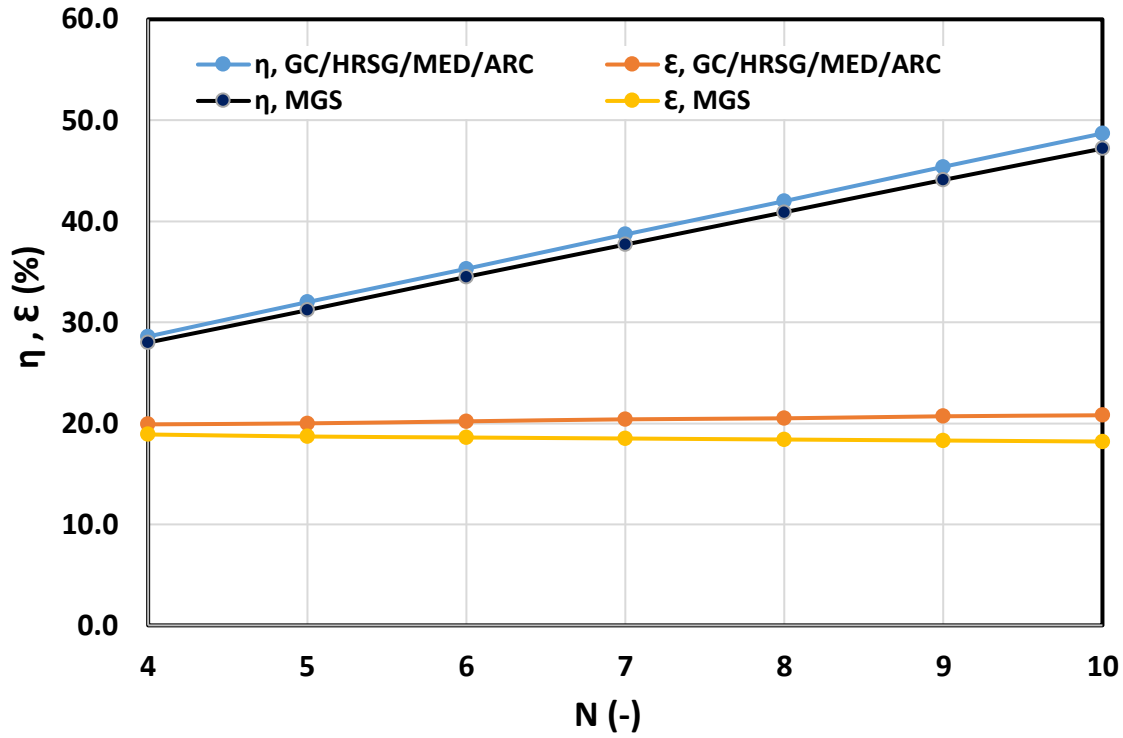
372

Figure 10. NPV, PP, IRR for GC, GC/HRSG/ARC/MED, and total system

373 **4.3. Parametric study**

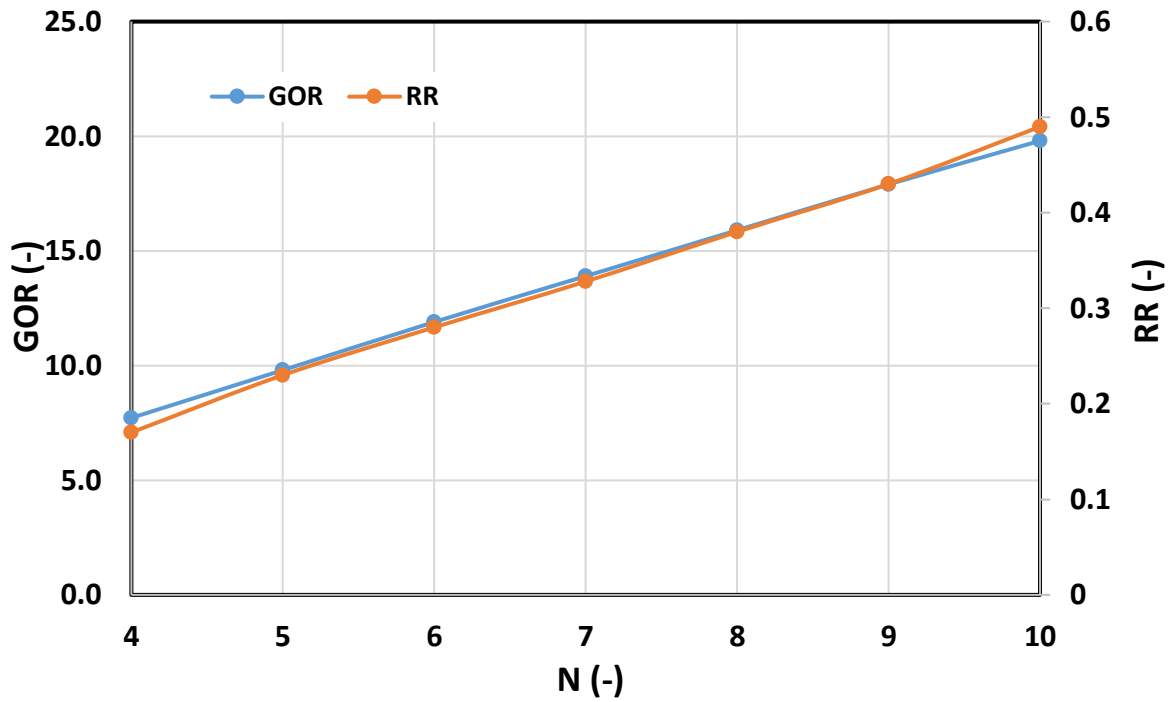
374 Figure 11 shows the variation of GC/HRSG/MED/ARC and MGS, ENE, and exergy efficiency versus the
 375 number of effects (N). It is clear that by increasing N from 4 to 10, GC/HRSG/MED/ARC ENE is increased
 376 from 28.6% to 48.7%. Also, the MGS ENE increased from 28% to 47.2%. It can be concluded that N has a
 377 considerable effect on the system performance improvement from the energy point of view. The effect
 378 of increasing N on GC/HRSG/MED/ARC and MGS exergy efficiency is not considerable. This means that
 379 GC/HRSG/MED/ARC exergy efficiency is only increased from 19.9% to 20.8% by increasing N from 4 to 10.
 380 For the MGS exergy efficiency, the inverse trend is observed. That is, by increasing N from 4 to 10, the
 381 MGS EXE is decreased from 18.9% to 18.2%. The reason for this phenomenon is that the specific exergy
 382 of DW, NaOH, and HCl is low. Figure 12 shows the variation of GOR and RR of MED with N. Both of these
 383 factors are increased with increasing N and this increase is nearly linear. Although the increase of N is
 384 beneficial for the production of higher DW, economic and technical restrictions are noted. The value of N
 385 should be calculated and justified based on DW needs, budget, etc.

386



387

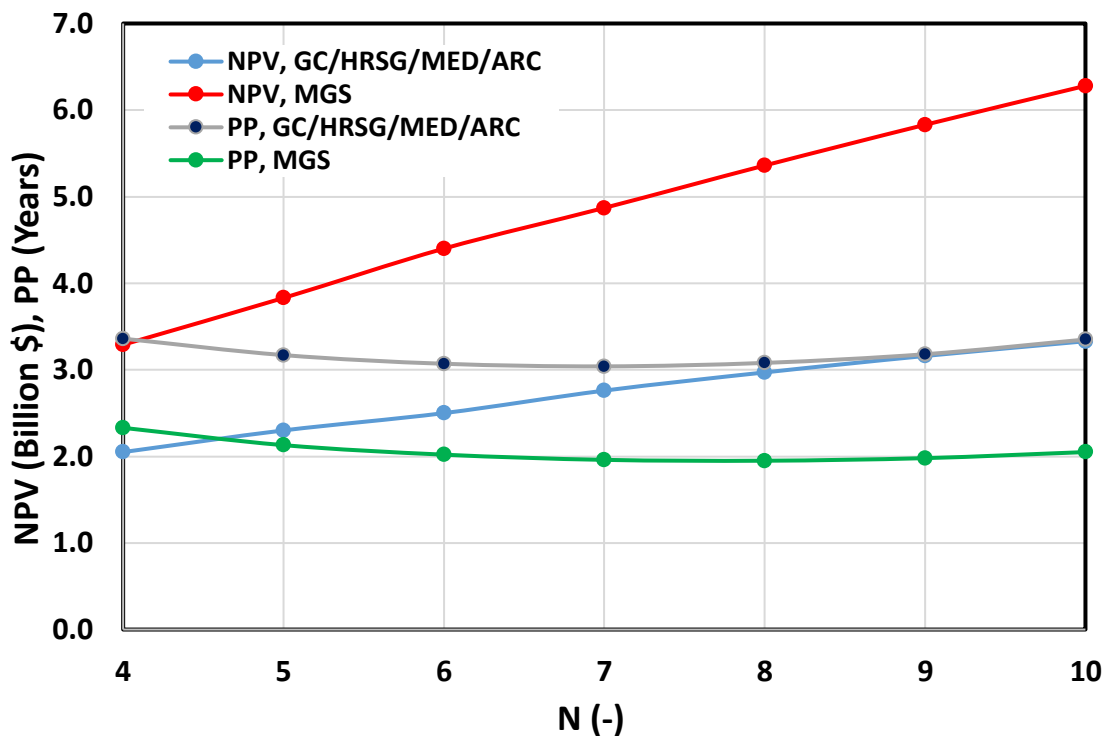
388 Figure 11. Variation of GC/HRSG/MED/ARC and MGS energy and exergy efficiencies versus the number
 389 of effects (N)



390

391 Figure 12. Variation of GOR and RR of MED with N

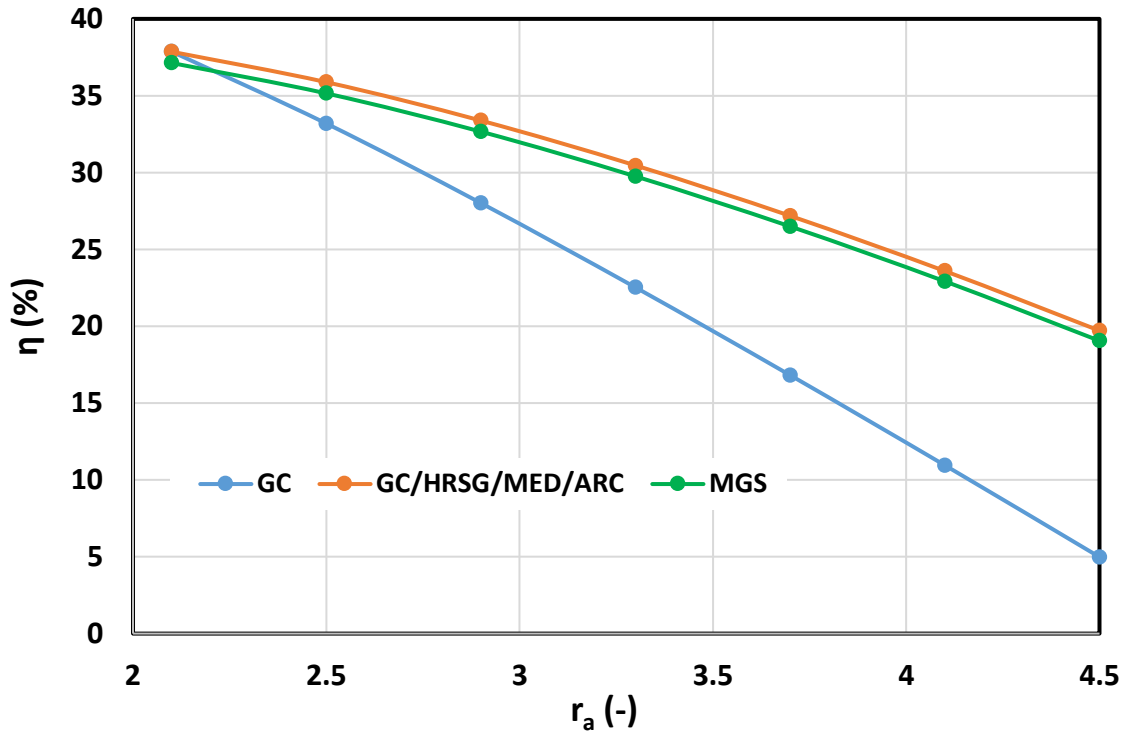
392 Figure 13 shows the variation of NPV and PP for GC/HRSG/MED/ARC and MGS with N. Increasing N from
 393 4 to 10 causes an increase in NPV in both cases. The percentage increases of NPV for GC/HRSG/MED/ARC
 394 and MGS are 62.4% and 91%, respectively. The PP of GC/HRSG/MED/ARC and MGS are reduced from 3.4
 395 and 2.3 years to 3.3 and 2.1 years, respectively.



396
 397 Figure 13. Variation of NPV and PP for GC/HRSG/MED/ARC and MGS with N

398 The variation of ENE of GC, GC/HRSG/MED/ARC, and MGS with r_a is presented in Figure 14. Increasing r_a
 399 causes a reduction of ENE in all three cases. For GC, this decrease is more than for the two other systems.
 400 Increasing r_a results in increasing the CC exhaust HOT gas mass flow rate and decreasing the CC
 401 temperature.

402 The first effect causes an increase in the net power production of the GC while the second leads to an
 403 opposite effect. Integration of GC with HRSG/MED/ARC dampens this considerable reduction of ENE since
 404 a higher exhaust hot gas mass flow rate from the GT increases the heat transfer rate in the HRSG and
 405 causes more steam production in the HRSG than is used in the MED for DW production. The trend of
 406 GC/HRSG/MED/ARC is similar to that for MGS.



407

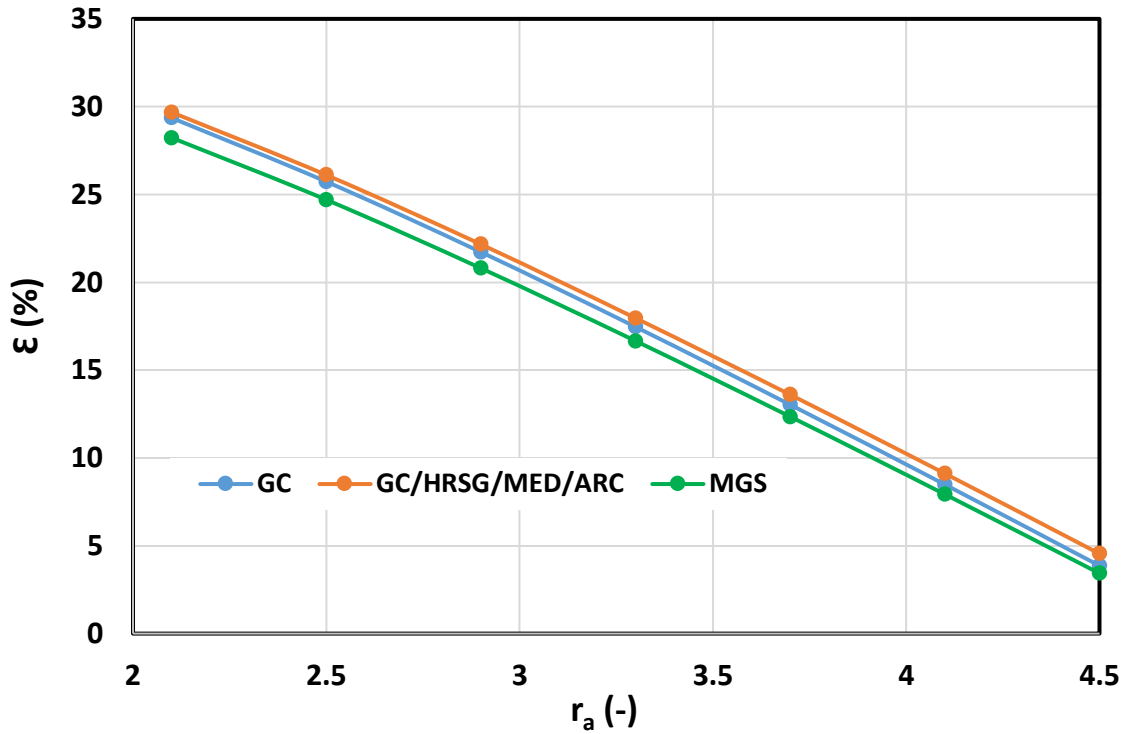
408

Figure 14. Variation of ENE of GC, GC/HRSG/MED/ARC, and MGS with r_a

409

Figure 15 shows the variation of exergy efficiency of GC, GC/HRSG/MED/ARC, and MGS versus r_a . Similar to Figure 14, increasing r_a causes a reduction in exergy efficiency in all three cases. The slope of reduction for exergy efficiency is also much higher than for ENE, of the three considered systems.

412



413

414 Figure 15. Variation of exergy efficiency of GC, GC/HRSR/MED/ARC, and MGS versus r_a

415 The variation of PP in the three cases (GC, GC/HRSR/MED/ARC, and MGS) versus r_a is shown in Figure 17.

416 The PP in all three cases is increased since TC increases due to increasing the size of components.

417 Considering Figure 15, ENE in all three cases is also reduced. Considering these two reasons, PP is

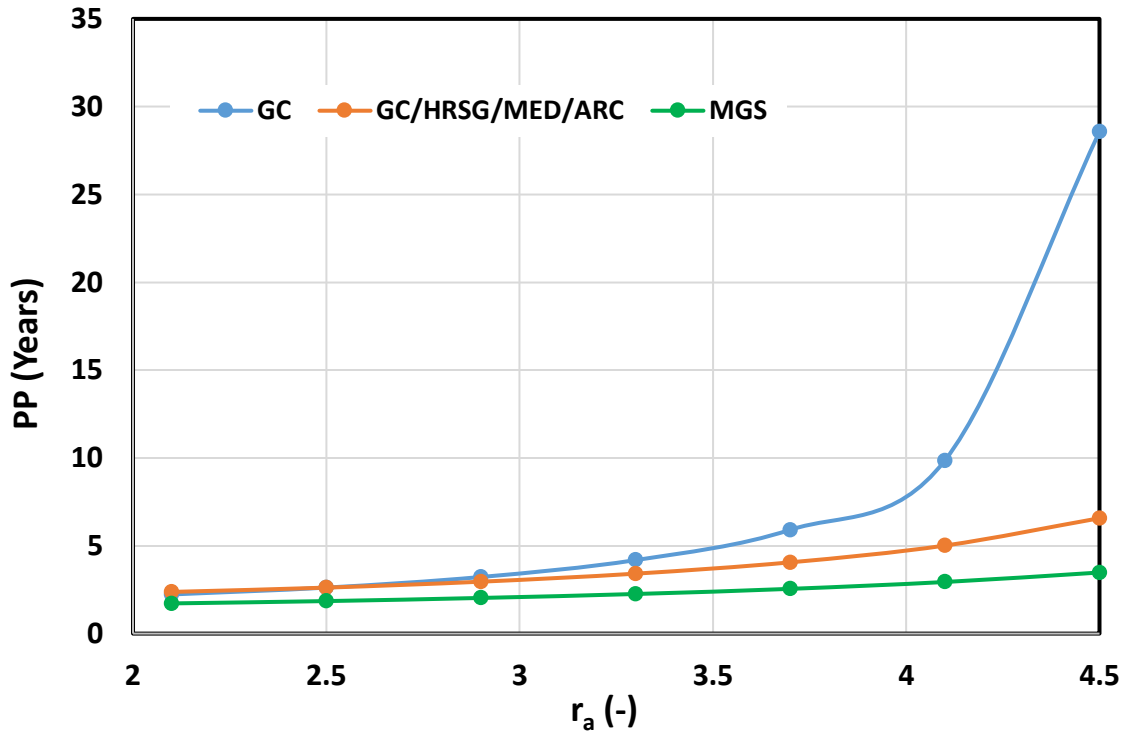
418 increased in all three cases. The slope of the curve is higher for GC in comparison with

419 GC/HRSR/MED/ARC, and MGS. For example, when increasing r_a from 2.1 to 4.5, the PP of GC is increased

420 from 2.2 to 28.6 years. For GC/HRSR/MED/ARC and MGS systems, the PP is 6.6 and 3.5 years, respectively,

421 which is much lower than for GC, since in these cases, increasing r_a helps to increase the MED and ELECD

422 product outputs.

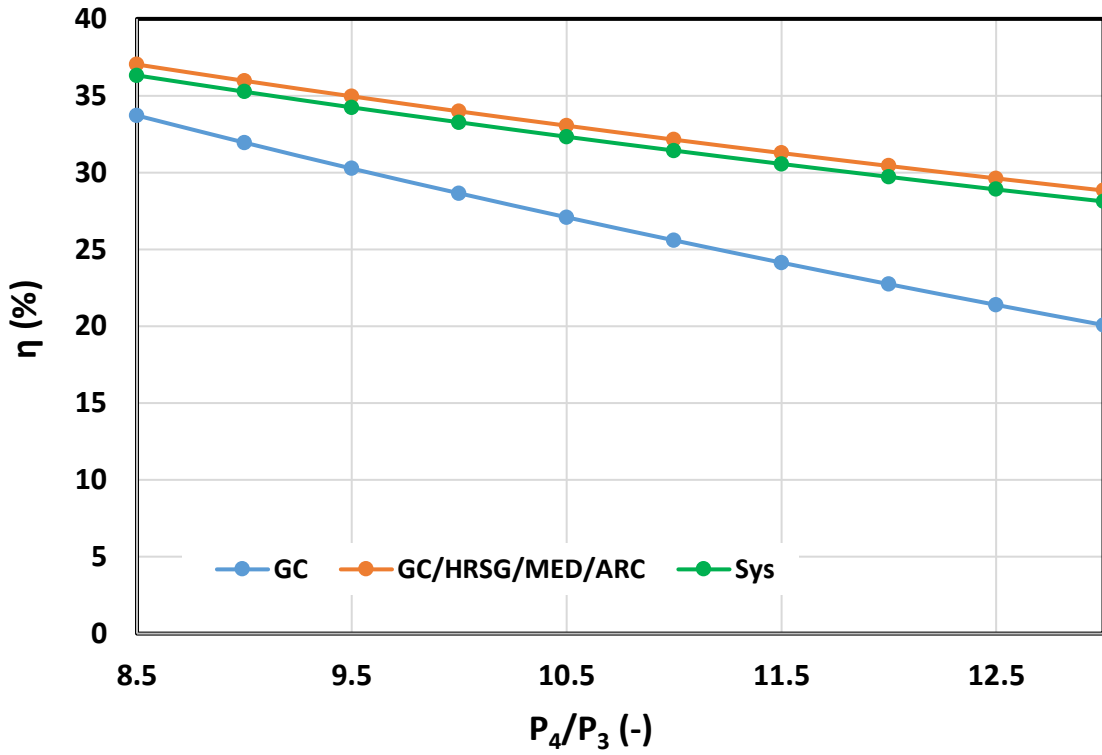


423

424 Figure 16. Variation of PP in three cases GC, GC/HRSG/MED/ARC, and MGS versus r_a

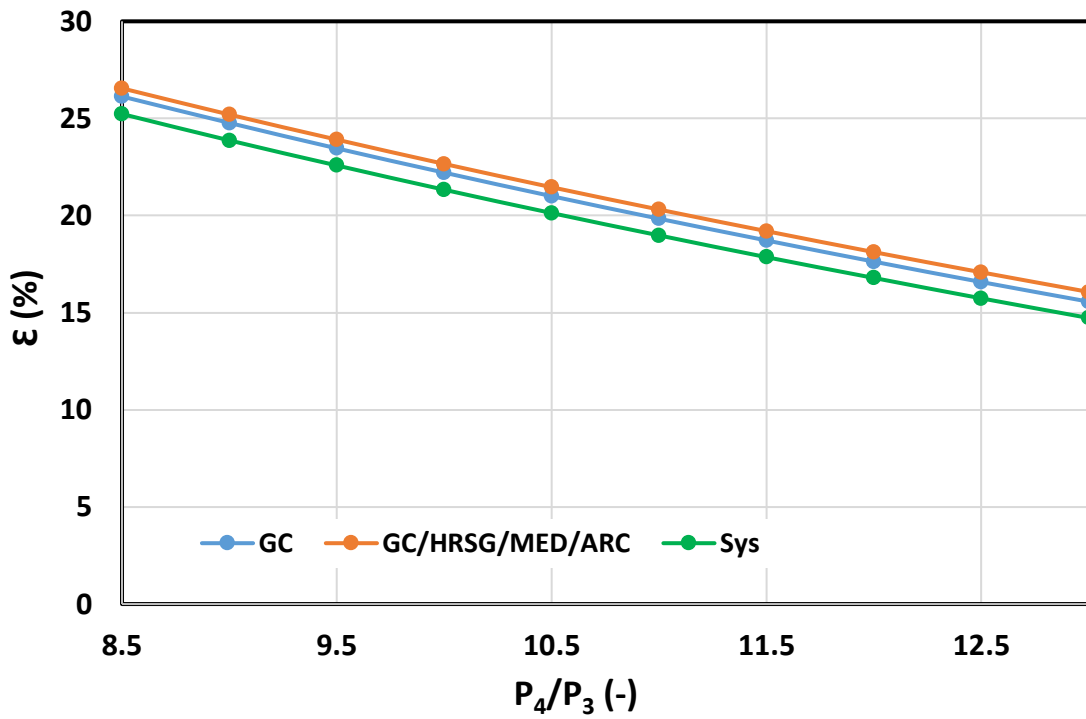
425 Figure 17 shows the variation of GC, GC/HRSG/MED/ARC, and MGS energy efficiency with compressor
 426 pressure ratio. It seems that increasing the compressor pressure ratio is not beneficial due to the
 427 reduction in ENE. The compressor pressure ratio cannot be selected as low as possible since the GT power
 428 production is reduced. The selected GT expansion ratio is slightly lower than the compressor pressure
 429 ratio for avoiding backflow in the exhaust of GT. The variation of GC, GC/HRSG/MED/ARC, and MGS exergy
 430 efficiency versus compressor pressure ratio is depicted in Figure 18. The trend of the exergy efficiency
 431 evolution is similar to that for ENE (Figure 17).

432



433

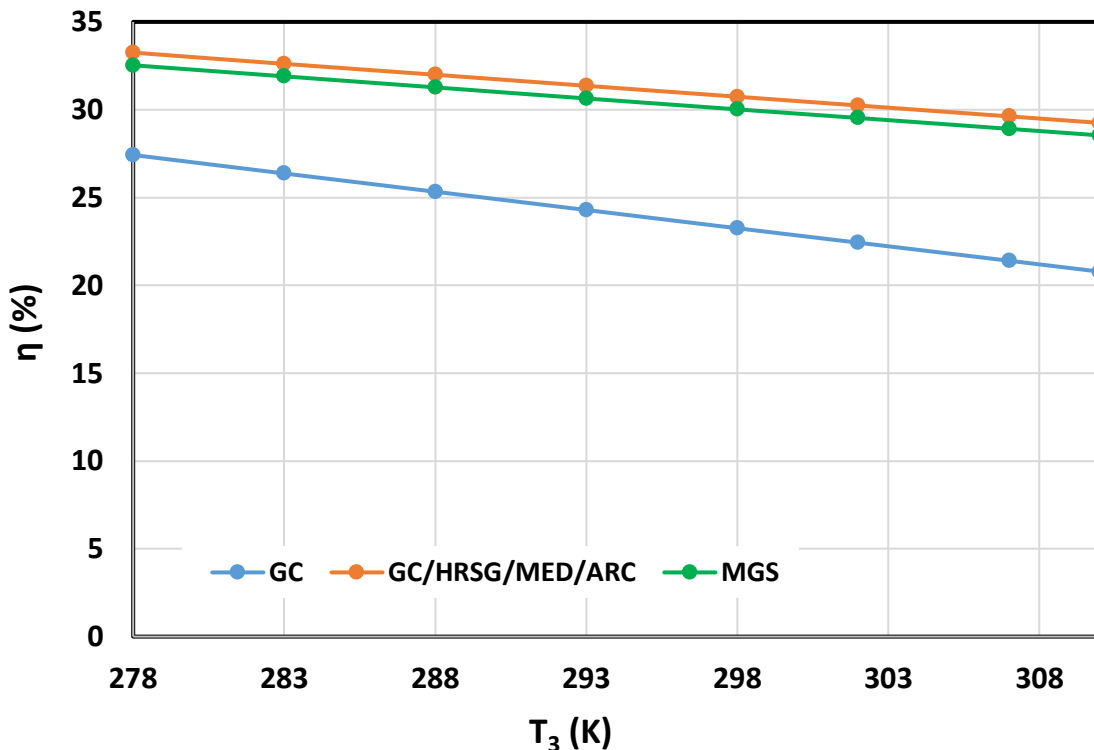
434 Figure 17. Variation of GC, GC/HRSG/MED/ARC, and MGS energy efficiency with compressor pressure
435 ratio



436

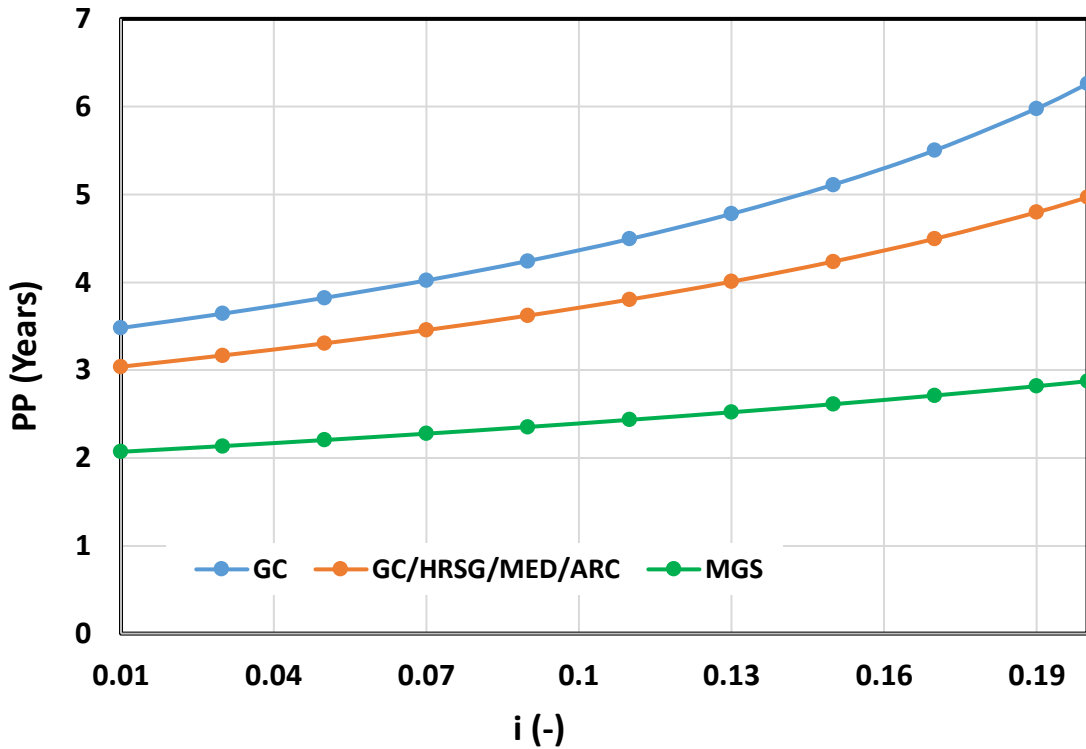
437 Figure 18. Variation of GC, GC/HRSG/MED/ARC, and MGS exergy efficiency with compressor pressure
438 ratio

439 Figure 19 shows the variation of ENE for GC, GC/HRSG/MED/ARC, and MGS energy efficiency versus air
 440 temperature. For the GC, the design is based on a constant volumetric flow rate. So, increasing air
 441 temperature causes a reduction in air density. Decreasing air density causes a reduction in air mass flow
 442 rate, power production, ENE, and exergy efficiency of the GC. This phenomenon has been reported
 443 elsewhere [14, 16, 68]. Considering Figure 20, the integration of GC with HRSG/MED/ARC as well as ELECD
 444 cannot offset entirely the reduction of exergy efficiency due to increasing air temperature, but it can
 445 dampen it. When increasing air temperature from 278 K to 310 K, the GC energy efficiency is reduced by
 446 around 24% while it is reduced to 12% for MGS.



447
 448 Figure 19. Variation of ENE for GC, GC/HRSG/MED/ARC, and MGS energy efficiency versus air
 449 temperature

450 Figure 20 shows the variation of PP for GC, GC/HRSG/MED/ARC, and MGS with inflation rate (i). By
 451 increasing the inflation rate from 1% to 20%, the PP of MGS is increased from 2.07 to 2.87 years. This
 452 increase is the highest for the GC, at 79.8%. For the GC/HRSG/MED/ARC configuration, PP increases by
 453 around 63%. By comparing the percentages of PP increasing, it can be concluded that integrating GC with
 454 other subsystems can overcome the effect of the inflation rate.



455

456 Figure 20. Variation of PP for GC, GC/HRSG/MED/ARC, and MGS with inflation rate (i)

457 **4. Conclusions**

458 In this study, a new MGS configuration was proposed and evaluated by energy, exergy, and economic
 459 analyses. The products of this system are electricity, cooling, DW, NaOH, and HCl. This proposed system
 460 included GC, SC, ARC, HRSG, MED, and ELECD. The ELECD is used in this proposed system to produce useful
 461 products and avoid the release of brine into the marine ecosystem. With this configuration, the proposed
 462 system becomes more environmentally friendly. It is clear that, if superheated steam produced in HRSG
 463 is used in the steam cycle to produce electricity, the MGS ENE and exergy efficiency are improved.
 464 Decision-making about the products of an MGS is based on the needs of customers and investors
 465 considering that the point is to purchase their products and the promotion of enhanced energy and exergy
 466 efficiencies for the MGS.

467 The main findings of this paper are as follows:

- 468 • The MGS produced 614.7 GWh of electrical energy, 87.44 GWh of cooling, 12.48 million m³ of DW,
 469 0.092 million tonnes of NaOH, and 0.084 million tonnes of HCl
- 470
- 471 • Integration of HRSG/MED/ARC to GC improved ENE from 25.3% to 32% while adding the ELECD
 472 decreased slightly the ENE from 32% to 31.3%.

- 473
- 474 • Integration of HRSG/MED/ARC to GC improved slightly exergy efficiency from 19.6% to 20% while
- 475 adding the ELECD decreased the exergy efficiency from 20% to 18.7%.
- 476
- 477 • The CC and MED feature the highest percentage of EDR while P1, BC, and GT exhibit the lowest
- 478 percentage of EDR.
- 479
- 480 • The integration of ELECD to the GC/HRSG/MED/ARC configuration decreases PP from 3.2 to 2.1
- 481 years while the integration of HRSG/MED/ARC to GC does not have a considerable effect on PP
- 482 improvement. Integration of ELECD to GC/HRSG/MED/ARC is strongly recommended from an
- 483 economic point of view.
- 484

485 The following future research is merited:

- 486 • Integration of GC with SOFC can be attractive while other subsystems can be the same as in the
- 487 present work.
- 488 • Superheated steam produced in HRSG is used for electrical production in the steam turbine. The
- 489 produced electricity can be fed to RO to produce PW. This system can then be compared with the
- 490 present work.
- 491 • Renewable energy resources can be attractive for producing superheated steam via concentrating
- 492 solar technologies. This superheated steam can be used in MED, while the other subsystems are
- 493 the same as in the present work.
- 494 • Evaluation and calculation of the social cost of releasing brine to the environment and life cycle
- 495 analysis of the proposed MGS.

496

497

498

499 **Nomenclature**

Acronyms

ABC	Air bottom cycle
ARC	Absorption refrigeration cycle
BC	Booster compressor
C	Compressor
CC	Combined cycle/Combustion chamber
DS	Dissolved solids
DV	Distillate vapor
DW	Distilled water
EDR	Exergy destruction rate
ELECD	Electrodialysis

ENE	Energy efficiency
FO	Forward osmosis
G	Generator
GA	Genetic algorithm
GC	Gas cycle
GT	Gas turbine
HDH	Humidification-dehumidification
HRSO	Heat recovery steam generator
LMTD	Logarithmic mean temperature difference
MD	Membrane distillation
MED	Multi-effect distillation
MGS	Multigeneration system
MSF	Multi-stage flash
NEA	Non-equilibrium allowance
NG	Natural gas
ORC	Organic Rankine cycle
P	Pump
PTC	Parabolic through collector
PW	Potable water
RC	Rankine cycle
RO	Reverse osmosis
SC	Steam cycle
SER	Steam ejector refrigerator
SOFC	Solid oxide fuel cell
SW	Seawater
TPC	Total product cost
TVC	Thermal vapor compressor

Symbols

A	Surface area (m ²)
AI	Annual income (US\$)
BBT	Bottom brine temperature (°C)
BPE	Boiling point elevation (°C)

c	Specific cost of products (US\$/kWh) or (US\$/kg) or (US\$/m ³)
COP	Coefficient of performance (-)
CSA	Civil, structural, and architectural work costs (US\$)
DC	Direct cost (US\$)
E	Electrical equipment and materials cost (US\$)
E&S	Engineering and supervision cost (US\$)
ff	Flashing fraction (-)
g	Gravitational acceleration (m/s ²)
GOR	Gained output ratio (-)
h	Specific enthalpy (kJ/kg)
i	Inflation rate (-)
IC	Indirect cost (US\$)
I&C	Instrumentation and controls cost (US\$)
IRR	Internal rate of return (-)
L	Latent heat (kJ/kg) or cost of land (US\$)
LHV	Lower heating value (kJ/kg)
\dot{m}	Mass flow rate (kg/s)
N	Number of effects (-)
N	Lifetime of the project (years)
n	Number of years (-)
NEA	Non-equilibrium allowance (°C)
OC	Other costs (US\$)
OMC	Operation and maintenance cost (US\$)
P	Pressure (kPa)
PEC	Purchased equipment cost (\$)
PEI	Purchased-equipment installation (US\$)
PI	Piping (US\$)
PP	Payback period (years)
\dot{Q}	Heat transfer rate (kW)
R	Universal gas constant, R=8.314 (kJ/kmol.K)
r	Discount factor (-)
r _a	Air-to-fuel ratio (-)

Ra	The ratio of entrained steam to motive steam (-)
RR	Recovery ratio (-)
s	Specific entropy (kJ/kg.K)
S&C	Startup costs (US\$)
SF	Service facilities cost (US\$)
T	Temperature (°C or K)
TBT	Top brine temperature (°C)
TC	Total cost (US\$)
TCI	Total capital investment (US\$)
U	Overall heat transfer coefficient (W/m ² K)
V	Velocity (m/s)
WC	Working capital cost (US\$)
\dot{W}	Work transfer rate (kW)
x	Salt concentration (-)
x	Mass fraction (-)
y	Mole fraction (-)
Y	Annual capacity (kWh/year) or (kg/year) or (m ³ /year)
z	Height (m)

Greek symbols

η	Energy efficiency (-)
ε	Exergy efficiency (-)
Ψ	Specific exergy (kJ/kg)

Subscripts

0	Dead state
BC	Booster compressor
C	Compressor
CC	Combined cycle/Combustion chamber
ch	Chemical
cond	Condenser
DV	Distillate vapor
DW	Distilled water

elec	Electrical
ELECD	Electrodialysis
GT	Gas turbine
HX	Heat exchanger
i	Species, Inlet flow
m	Motive steam
N	Effects number
NG	Natural gas
P	Pump
ph	Preheater
s	Steam
SW	Seawater
v	Vapor

500

501

502 **References**

503 [1] Overview of water scarcity See: worldwildlife.org/threats/water-scarcity

504 2021.

505 [2] P.I. Peter H. Gleick, Newsha Ajami, Juliet Christian-Smith, Heather Cooley, Kristina Donnelly, Julian
506 Fulton, Mai-Lan Ha, Matthew Heberger, Eli Moore, Jason Morrison, Stewart Orr, Peter Schulte, and Veena
507 Srinivasan. The World's Water The Biennial Report on Freshwater Resources. 8 (2021) 496.

508 [3] Z. Huang, X. Liu, S. Sun, Y. Tang, X. Yuan, Q. Tang. Global assessment of future sectoral water scarcity
509 under adaptive inner-basin water allocation measures. Science of The Total Environment. 783 (2021)
510 146973.

511 [4] H. Cooley, P.H. Gleick, G.H. Wolff. Desalination, with a grain of salt: a California perspective. Pacific
512 Institute for Studies in Development, Environment, and Security ...2006.

513 [5] M. Islam, A. Sultana, A. Saadat, M. Shammi, M. Uddin. Desalination technologies for developing
514 countries: A review. Journal of Scientific Research. 10 (2018) 77-97.

515 [6] M.A. Ehyaei, S. Baloochzadeh, A. Ahmadi, S. Abanades. Energy, exergy, economic,
516 exergoenvironmental, and environmental analyses of a multigeneration system to produce electricity,
517 cooling, potable water, hydrogen and sodium-hypochlorite. Desalination. 501 (2021) 114902.

518 [7] W.L. Ang, A. Wahab Mohammad, D. Johnson, N. Hilal. Forward osmosis research trends in desalination
519 and wastewater treatment: A review of research trends over the past decade. Journal of Water Process
520 Engineering. 31 (2019) 100886.

521 [8] F.A. AlMarzooqi, A.A. Al Ghaferi, I. Saadat, N. Hilal. Application of Capacitive Deionisation in water
522 desalination: A review. Desalination. 342 (2014) 3-15.

523 [9] A. Alkhudhiri, N. Hilal. 3 - Membrane distillation—Principles, applications, configurations, design, and
524 implementation. in: V.G. Gude, (Ed.). Emerging Technologies for Sustainable Desalination Handbook.
525 Butterworth-Heinemann 2018. pp. 55-106.

526 [10] F.E. Ahmed, R. Hashaikeh, N. Hilal. Solar powered desalination – Technology, energy and future
527 outlook. *Desalination*. 453 (2019) 54-76.

528 [11] O.M.A. Al-Hotmani, M.A.A. Al-Obaidi, Y.M. John, R. Patel, I.M. Mujtaba. Scope and Limitations of the
529 Mathematical Models Developed for the Forward Feed Multi-Effect Distillation Process—A Review.
530 *Processes*. 8 (2020) 1174.

531 [12] A. Panagopoulos, K.-J. Haralambous, M. Loizidou. Desalination brine disposal methods and treatment
532 technologies - A review. *Science of The Total Environment*. 693 (2019) 133545.

533 [13] N. Heck, K. Lykkebo Petersen, D.C. Potts, B. Haddad, A. Paytan. Predictors of coastal stakeholders'
534 knowledge about seawater desalination impacts on marine ecosystems. *Science of The Total
535 Environment*. 639 (2018) 785-92.

536 [14] M.R.M. Yazdi, M. Aliehyaei, M.A. Rosen. Exergy, economic and environmental analyses of gas turbine
537 inlet air cooling with a heat pump using a novel system configuration. *Sustainability*. 7 (2015) 14259-86.

538 [15] S. Safari, T. Hajilounezhad, M.A. Ehyaei. Multi-objective optimization of solid oxide fuel cell/gas
539 turbine combined heat and power system: A comparison between particle swarm and genetic algorithms.
540 *International Journal of Energy Research*. 44 (2020) 9001-20.

541 [16] M.A. Ehyaei, S. Hakimzadeh, N. Enadi, P. Ahmadi. Exergy, economic and environment (3E) analysis of
542 absorption chiller inlet air cooler used in gas turbine power plants. *International Journal of Energy
543 Research*. 36 (2012) 486-98.

544 [17] M.R. Majdi Yazdi, F. Ommi, M.A. Ehyaei, M.A. Rosen. Comparison of gas turbine inlet air cooling
545 systems for several climates in Iran using energy, exergy, economic, and environmental (4E) analyses.
546 *Energy Conversion and Management*. 216 (2020) 112944.

547 [18] M.A. Ehyaei, M. Tahani, P. Ahmadi, M. Esfandiari. Optimization of fog inlet air cooling system for
548 combined cycle power plants using genetic algorithm. *Applied Thermal Engineering*. 76 (2015) 449-61.

549 [19] A. Ahmadi, D.H. Jamali, M.A. Ehyaei, M.E.H. Assad. Energy, exergy, economic and
550 exergoenvironmental analyses of gas and air bottoming cycles for production of electricity and hydrogen
551 with gas reformer. *Journal of Cleaner Production*. 259 (2020) 120915.

552 [20] S. Alizadeh, A. Ghazanfari, M. Ehyaei, A. Ahmadi, D. Jamali, N. Nedaei, et al. Investigation the
553 integration of heliostat solar receiver to gas and combined cycles by energy, exergy, and economic point
554 of views. *Applied Sciences*. 10 (2020) 5307.

555 [21] M. Shamoushaki, M.A. Ehyaei, F. Ghanatir. Exergy, economic and environmental analysis and multi-
556 objective optimization of a SOFC-GT power plant. *Energy*. 134 (2017) 515-31.

557 [22] G. Fan, A. Ahmadi, M.A. Ehyaei, B. Das. Energy, exergy, economic and exergoenvironmental analyses
558 of polygeneration system integrated gas cycle, absorption chiller, and Copper-Chlorine thermochemical
559 cycle to produce power, cooling, and hydrogen. *Energy*. 222 (2021) 120008.

560 [23] M. Shakouri, H. Ghadamian, R. Sheikholeslami. Optimal model for multi effect desalination system
561 integrated with gas turbine. *Desalination*. 260 (2010) 254-63.

562 [24] H. Mokhtari, M. Sepahvand, A. fasihfar. Thermoeconomic and exergy analysis in using hybrid systems
563 (GT+MED+RO) for desalination of brackish water in Persian Gulf. *Desalination*. 399 (2016) 1-15.

564 [25] T. Renonnet, J. Uche, L. Serra. Simulation and thermoeconomic analysis of different configurations
565 of gas turbine (GT)-based dual-purpose power and desalination plants (DPPDP) and hybrid plants (HP).
566 *Energy*. 32 (2007) 1012-23.

567 [26] P. Ahmadi, S. Khanmohammadi, F. Musharavati, M. Afrand. Development, evaluation, and multi-
568 objective optimization of a multi-effect desalination unit integrated with a gas turbine plant. *Applied
569 Thermal Engineering*. 176 (2020) 115414.

570 [27] A. Mohammadnia, A. Asadi. A hybrid solid oxide fuel cell-gas turbine fed by the motive steam of a
571 multi-effects desalination-thermo vapor compressor system. *Energy Conversion and Management*. 216
572 (2020) 112951.

573 [28] R. Ahmadi, S.M. Pourfatemi, S. Ghaffari. Exergoeconomic optimization of hybrid system of GT, SOFC
574 and MED implementing genetic algorithm. *Desalination*. 411 (2017) 76-88.

575 [29] N. Nazari, S. Porkhial. Multi-objective optimization and exergo-economic assessment of a solar-
576 biomass multi-generation system based on externally-fired gas turbine, steam and organic Rankine cycle,
577 absorption chiller and multi-effect desalination. *Applied Thermal Engineering*. 179 (2020) 115521.

578 [30] H. You, J. Han, Y. Liu. Performance assessment of a CCHP and multi-effect desalination system based
579 on GT/ORC with inlet air precooling. *Energy*. 185 (2019) 286-98.

580 [31] M. Moghimi, M. Emadi, A. Mirzazade Akbarpoor, M. Mollaei. Energy and exergy investigation of a
581 combined cooling, heating, power generation, and seawater desalination system. *Applied Thermal
582 Engineering*. 140 (2018) 814-27.

583 [32] K.H. Mistry, M.A. Antar, J.H. Lienhard V. An improved model for multiple effect distillation.
584 *Desalination and Water Treatment*. 51 (2013) 807-21.

585 [33] A. Bejan. *Advanced engineering thermodynamics*. John Wiley & Sons, Hoboken, New Jersey, 2016.

586 [34] A. Mozafari, A. Ahmadi, M. Ehyaei. Optimisation of micro gas turbine by exergy, economic and
587 environmental (3E) analysis. *International Journal of Exergy*. 7 (2010) 1-19.

588 [35] F.N. Alasfour, M.A. Darwish, A.O. Bin Amer. Thermal analysis of ME-TVC+MEE desalination systems.
589 *Desalination*. 174 (2005) 39-61.

590 [36] I.S. Al-Mutaz, I. Wazeer. Development of a steady-state mathematical model for MEE-TVC
591 desalination plants. *Desalination*. 351 (2014) 9-18.

592 [37] O. Miyatake, K. Murakami, Y. Kawata, T. Fujii. Fundamental experiments with flash evaporation. *Heat
593 Transfer-Jpn Res*. 2 (1973) 89-100.

594 [38] H.T. El-Dessouky, H.M. Ettouney. *Fundamentals of salt water desalination*. Elsevier 2002.

595 [39] F.N. Alasfour, M.A. Darwish, A.O. Bin Amer. Thermal analysis of ME—TVC+MEE desalination systems.
596 *Desalination*. 174 (2005) 39-61.

597 [40] H. El-Dessouky, H. Ettouney, F. Al-Juwayhel. Multiple effect evaporation—vapour compression
598 desalination processes. *Chemical Engineering Research and Design*. 78 (2000) 662-76.

599 [41] J. Liu, L. Wang, L. Jia, H. Xue. Thermodynamic analysis of the steam ejector for desalination
600 applications. *Applied Thermal Engineering*. 159 (2019).

601 [42] G.P. Thiel, A. Kumar, A. Gómez-González, J.H. Lienhard. Utilization of desalination brine for sodium
602 hydroxide production: technologies, engineering principles, recovery limits, and future directions. *ACS
603 Sustainable Chemistry & Engineering*. 5 (2017) 11147-62.

604 [43] A. Lazzaretto, G. Tsatsaronis. SPECO: a systematic and general methodology for calculating
605 efficiencies and costs in thermal systems. *Energy*. 31 (2006) 1257-89.

606 [44] A. Bejan, G. Tsatsaronis, M. Moran. *Thermal Design and Optimization* John Wiley and Sons. Inc New
607 York. (1996).

608 [45] E. Bellos, S. Pavlovic, V. Stefanovic, C. Tzivanidis, B.B. Nakomcic-Smaradgakis. Parametric analysis and
609 yearly performance of a trigeneration system driven by solar-dish collectors. *International Journal of
610 Energy Research*. 43 (2019) 1534-46.

611 [46] C. Tzivanidis, E. Bellos, K.A. Antonopoulos. Energetic and financial investigation of a stand-alone solar-
612 thermal Organic Rankine Cycle power plant. *Energy conversion and management*. 126 (2016) 421-33.

613 [47] P. Prebeg, G. Gasparovic, G. Krajacic, N. Duic. Long-term energy planning of Croatian power system
614 using multi-objective optimization with focus on renewable energy and integration of electric vehicles.
615 *Applied Energy*. 184 (2016) 1493-507.

616 [48] M. Castaneda, A. Cano, F. Jurado, H. Sánchez, L.M. Fernandez. Sizing optimization, dynamic modeling
617 and energy management strategies of a stand-alone PV/hydrogen/battery-based hybrid system.
618 International Journal of Hydrogen Energy. 38 (2013) 3830-45.

619 [49] H. Nami, I.S. Ertesvåg, R. Agromayor, L. Riboldi, L.O. Nord. Gas turbine exhaust gas heat recovery by
620 organic Rankine cycles (ORC) for offshore combined heat and power applications-Energy and exergy
621 analysis. Energy. 165 (2018) 1060-71.

622 [50] H. Nami, E. Akrami. Analysis of a gas turbine based hybrid system by utilizing energy, exergy and
623 exergoeconomic methodologies for steam, power and hydrogen production. Energy Conversion and
624 Management. 143 (2017) 326-37.

625 [51] M. Temiz, I. Dincer. Concentrated solar driven thermochemical hydrogen production plant with
626 thermal energy storage and geothermal systems. Energy. 219 (2021) 119554.

627 [52] Sodium hydroxide See:pharmacompass.com/active-pharmaceutical-ingredients/sodium-hydroxide.
628 2021.

629 [53] Hydrochloric Acid See:pharmacompass.com/active-pharmaceutical-ingredients/hydrochloric-acid.
630 2021.

631 [54] P. Roosen, S. Uhlenbruck, K. Lucas. Pareto optimization of a combined cycle power system as a
632 decision support tool for trading off investment vs. operating costs. International Journal of Thermal
633 Sciences. 42 (2003) 553-60.

634 [55] M.D. Schöpfer. Absorption chillers: their feasibility in district heating networks and comparison to
635 alternative technologies. Master of Science Degree in Energy Engineering and Management. Technical
636 University of Lisbon. Technico Lisboa, Technico Lisboa university, 2015. p. 98.

637 [56] M. Gebhardt, H. Kohl, T. Steinrötter. Preisatlas, Ableitung von Kostenfunktionen für Komponenten
638 der rationellen Energienutzung. Institut für Energie und Umwelttechnik eV (IUTA). (2002) 1-356.

639 [57] J.L. Silveira, C.E. Tuna. Thermo-economic analysis method for optimization of combined heat and
640 power systems. Part I. Progress in Energy and Combustion Science. 29 (2003) 479-85.

641 [58] M.L. Elsayed, O. Mesalhy, R.H. Mohammed, L.C. Chow. Exergy and thermo-economic analysis for
642 MED-TVC desalination systems. Desalination. 447 (2018) 29-42.

643 [59] A. Bejan, G. Tsatsaronis, M.J. Moran. Thermal design and optimization. John Wiley & Sons 1995.

644 [60] T. Shafer. Calculating inflation factors for cost estimates. City of Lincoln Transportation and Utilities
645 Project Delivery.

646 [61] Statista. Global inflation rate compared to previous year See:statista.com/statistics/256598/global-
647 inflation-rate-compared-to-previous-year/.

648 [62] S. Edalati, M. Ameri, M. Iranmanesh, H. Tarmahi, M. Gholampour. Technical and economic
649 assessments of grid-connected photovoltaic power plants: Iran case study. Energy. 114 (2016) 923-34.

650 [63] M. Shamoushaki, M. Ehyaei, F. Ghanatir. Exergy, economic and environmental analysis and multi-
651 objective optimization of a SOFC-GT power plant. Energy. 134 (2017) 515-31.

652 [64] M. Ehyaei, A. Mozafari, M. Alibiglou. Exergy, economic & environmental (3E) analysis of inlet fogging
653 for gas turbine power plant. Energy. 36 (2011) 6851-61.

654 [65] M. Ehyaei, S. Hakimzadeh, N. Enadi, P. Ahmadi. Exergy, economic and environment (3E) analysis of
655 absorption chiller inlet air cooler used in gas turbine power plants. International Journal of Energy
656 Research. 36 (2012) 486-98.

657 [66] M. Ghazikhani, N. Manshoori, D. Tafazoli. Influence of Steam Injection on Thermal Efficiency and
658 Operating Temperature of GE-F5 Gas Turbines Applying VODOLEY System. ASME 2005 International
659 Mechanical Engineering Congress and Exposition. American Society of Mechanical Engineers Digital
660 Collection 2005. pp. 217-24.

661 [67] A.L. Polyzakis, C. Koroneos, G. Xydis. Optimum gas turbine cycle for combined cycle power plant.
662 Energy Conversion and Management. 49 (2008) 551-63.

663 [68] M.A. Ehyaei, A. Mozafari, M.H. Alibiglou. Exergy, economic & environmental (3E) analysis of inlet
664 fogging for gas turbine power plant. Energy. 36 (2011) 6851-61.

665